Developmental Biology 357 (2011) 404–418

Contents lists available at ScienceDirect

Developmental Biology

journal homepage: www.elsevier.com/developmentalbiology

Pabp binds to the *osk* 3′UTR and specifically contributes to *osk* mRNA stability and oocyte accumulation

Paula Vazquez-Pianzola [a], Henning Urlaub [b], Beat Suter [a,*]

[a] Institute of Cell Biology, University of Bern, Baltzerstrasse 4, 3012 Bern, Switzerland
[b] Bioanalytical Mass Spectrometry Group, Max Planck Institute for Biophysical Chemistry, Am Fassberg 11, 37077 Göttingen, Germany

ARTICLE INFO

Article history:
Received for publication 2 March 2011
Revised 5 July 2011
Accepted 7 July 2011
Available online 14 July 2011

Keywords:
Pabp
Bicaudal-D
Egalitarian
oskar
mRNA transport
mRNA stability
Oogenesis
Translational control

ABSTRACT

RNA localization is tightly coordinated with RNA stability and translation control. Bicaudal-D (Bic-D), Egalitarian (Egl), microtubules and their motors are part of a *Drosophila* transport machinery that localizes mRNAs to specific cellular regions during oogenesis and embryogenesis. We identified the Poly(A)-binding protein (Pabp) as a protein that forms an RNA-dependent complex with Bic-D in embryos and ovaries. *pabp* also interacts genetically with *Bic-D* and, similar to *Bic-D, pabp* is essential in the germline for oocyte growth and accumulation of *osk* mRNA in the oocyte. In the absence of *pabp,* reduced stability of *osk* mRNA and possibly also defects in *osk* mRNA transport prevent normal oocyte localization of *osk* mRNA. *pabp* also interacts genetically with *osk* and lack of one copy of *pabp* $^{+}$ causes *osk* to become haploinsufficient. Moreover, pointing to a poly(A)-independent role, Pabp binds to A-rich sequences (ARS) in the *osk* 3′UTR and these turned out to be required *in vivo* for *osk* function during early oogenesis. This effect of *pabp* on *osk* mRNA is specific for this RNA and other tested mRNAs localizing to the oocyte are less and more indirectly affected by the lack of *pabp*.

Introduction

mRNA localization focuses expression of proteins to specific regions of a cell. Many processes from the budding of a yeast to the establishment of embryonic axes in metazoans and the migration of human neuronal cells depend on this type of cell polarization (Du et al., 2007; Vardy and Orr-Weaver, 2007). During transport mRNAs associate with proteins that control every step in the life cycle of the RNA. Together they form large ribonucleoprotein (RNP) complexes in which trans-acting factors control assembly, stability, translational and transport of localized RNAs. Microtubules and their motors are then involved in the transport of these complex structures.

In *Drosophila,* a dynein mediated minus-end transport machinery composed of the physically interacting Bicaudal-D (Bic-D) and Egalitarian (Egl) proteins plays a key role in oogenesis by localizing into and within the oocyte different mRNAs. These RNAs are required for oocyte determination and differentiation, and for the formation of anterior–posterior and dorsal–ventral polarity. In addition, the same machinery is also involved in apical transport of specific mRNAs that pattern the early embryo (Bullock, 2007; Claußen and Suter, 2005). During oocyte determination, a single cell among an interconnected cyst of sixteen germline cells differentiates into an oocyte. This process involves the preferential accumulation of specific messenger RNAs and proteins in this cell. The fifteen remaining cells adopt a nurse cell fate and provide the oocyte with the materials required for its growth. In loss-of-function *Bic-D* mutants, the transport of oocyte specific proteins and mRNAs (such as *osk*, *orb, Bic-D* and *fs(1)K10*) to the future oocyte is blocked, the oocyte fails to differentiate and all 16 cystocytes become polyploid nurse cells (Ran et al., 1994; Suter and Steward, 1991). *egl* mutant ovaries as well as wild type ovaries, treated with microtubule depolymerizing drugs, show the same phenotype as *Bic-D* (Schüpbach and Wieschaus, 1991; Theurkauf et al., 1993). In addition, *Bic-D*, *egl* and microtubules are also required for the establishment of the dorsal–ventral axis (d–v) of the egg chamber by the positioning of the oocyte nucleus to the future dorso-anterior corner of the oocyte (Koch and Spitzer, 1983; Mach and Lehmann, 1997; Swan et al., 1999; Swan and Suter, 1996) and by transporting from the nurse cells the mRNA of the transforming growth factor alpha-like molecule Gurken (Grk) that signals to the adjacent follicle cells to become the dorsoanterior follicle cells (Clark et al., 2007). The maternal anterior–posterior determinants *bicoid* (*bcd*) and *oskar* (*osk*) also use the Bic-D/Egl machinery for their export from the nurse cells to the oocyte and *Bic-D* is required for *osk* posterior localization during late oogenesis (Clark et al., 2007; Swan and Suter, 1996).

Abbreviations: ARS, A-rich sequences; Bic-D, Bicaudal-D; Egl, Egalitarian; EMSA, electromobility shift assays; FLP, flipase; FRT, Flip recombinase target; *grk*, *gurken*; IP, immunoprecipitation; *orb*, oo18 RNA-binding protein; *osk*, *oskar*; Pabp, poly(A)-binding protein; Stau, Staufen; UTR, untranslated region; RNP, ribonucleoprotein; mRNP, messenger ribonocleoprotein.

* Corresponding author. Fax: +41 31 631 38 66.
E-mail address: beat.suter@izb.unibe.ch (B. Suter).

0012-1606/$ – see front matter © 2011 Elsevier Inc. All rights reserved.
doi:10.1016/j.ydbio.2011.07.009

The current molecular model of function of this machinery is suggested by several studies in *Drosophila* and work done on the mammalian Bic-D homologous. These findings suggest that the Bic-D/Egl complex acts as a link between a microtubule-dependent dynein motor and various cargos since the mammalian homologues of Bic-D bind directly *in vitro* and associate *in vivo* with components of the dynein and dynactin complexes, and *Drosophila* Egl binds the Dynein light chain (Dlc) (Hoogenraad et al., 2001; Navarro et al., 2004). Recently Dienstbier et al. provided evidence that Egl, despite being not a canonical RNA binding protein, can bind directly to embryonic RNAs that localize apically, suggesting that Egl is the protein in the complex that links the molecular motors and Bic-D with the transported mRNAs (Dienstbier et al., 2009). However, it is still not clear whether Egl is a general link for all the mRNAs transported by this machinery or whether additional proteins are needed for the specificity of the interaction. The significance of this question further increases because there is no obvious homolog of Egl in humans, which may indicate that other modes of interaction are possible. As outlined before, the transport machinery is part of a bigger RNP complex that also controls translation of the transported mRNAs, insuring that protein synthesis is only activated once the mRNAs reach their final destination (Besse and Ephrussi, 2008). *osk* mRNP particles are a model for translation control during transport. *osk* is only translated once it reaches its final destination at the posterior cortex of the oocyte after stage 8 of oogenesis. Before this stage, *osk* mRNA is transported from the nurse cells into the oocyte in a translation dormant state. While the miRNA pathway plays a role in repressing *osk* translation during early oogenesis up to stage 6, between stages 6 and 9 a complex containing Bruno–Cup–eIF4E, which targets cap-dependent initiation of translation, as well as *osk* oligomerization seem responsible for the repression (Kugler and Lasko, 2009).

A growing number of evidences indicate that different mechanisms involving specific RNP complexes co-operate to control formation, transport, translation and probably also stability of the different mRNAs during RNA transport (Kelsey and Ephrussi, 2009). In the case of the Bic-D/Egl transport machinery our knowledge about the study of associated trans acting factors controlling the life cycle of transported mRNAs is, however, still very limited. To find additional trans acting factors that contribute to the regulation of the localization process either by linking this machinery to the RNAs or controlling assembly, translation repression or stability of the mRNAs during transport, we searched for RNA binding proteins that are in complex with Bic-D using immunoprecipitation and mass spectrometry analysis. Studying the role of one of the novel components of the Bic-D machinery, the Poly(A)-binding protein (Pabp), we found that it possess a novel and surprising role. Pabp, a well-established general translation factor, turned out to be essential and specifically required for the proper accumulation of *osk* mRNA in the oocyte during early oogenesis. Other mRNAs transported by the Bic-D localization machinery were, however, less affected by lack of *Pabp*. In addition, the stability of *osk* mRNA was reduced in the absence of *Pabp*. Underscoring the novelty of this specific function of Pabp, it seems to perform it in a poly(A)-independent manner.

Results

Pabp is associated with Bic-D in an RNA-dependent manner

To identify additional components of the Egl/Bic-D complex, we performed immunoprecipitations (IP) of embryo extracts using two monoclonal anti Bic-D antibodies that recognize different epitopes (Fig. 1A) (Suter and Steward, 1991). Beads alone and beads coupled to the unrelated anti-Cdk7 antibodies were used as controls for unspecific binding. The immunoprecipitated material was resolved by SDS-PAGE, stained with Coomassie blue, and the specific bands obtained in experiments with both anti-Bic-D antibodies were identified by mass spectrometry. In this way we identified Pabp (also called PABP55B and PABPC1) as a potential novel component of the Egl/Bic-D transport machinery (Figs. 1A, A').

To corroborate this interaction, we performed IP experiments with embryo extracts and different antibodies, and we analyzed the complex composition using western blots (Fig. 1B). Both anti-Bic-D antibodies, which recognize different epitopes, coimmunoprecipitated endogenous Bic-D, Pabp and Egl. However, addition of RNase A during the experiments prevented coimunoprecipitation of Pabp even though the RNase did not affect the stability of Pabp (Fig. 1B and Supplementary Fig. S1A). In reciprocal experiments, anti-Pabp antibodies coimmunoprecipitated endogenous Pabp along with Bic-D (Fig. 1B). As expected for an RNA-dependent interaction, the coimmunoprecipitation of Pabp along with Bic-D was stabilized by the presence of Mg^{2+} (Supplementary Fig. S1B). In contrast, and consistent with a direct interaction between Egl and Bic-D, the interaction between these two proteins, was not affected by incubation with RNase A (Fig. 1B). Control experiments using beads alone or an unrelated monoclonal antibody against a murine protein did not coimmunoprecipitate Bic-D, Egl or Pabp (Fig. 1B). The co-IP of Pabp with Bic-D antibodies was also confirmed using ovary extracts and S2 cell extracts expressing a V5-tagged Pabp (not shown, and Supplementary Fig. S1C). In this case, the interaction was again RNA-dependent. Co-IP of Pabp with anti Bic-D antibody was not observed when embryonic or S2 cell extracts were first immunodepleted for Bic-D. Because these extracts still contained high amounts of Pabp, these experiments show again that Pabp is not directly recognized by the two anti Bic-D antibodies (Fig. 1C and Supplementary Fig. S1C). Pabp therefore seems to be a component of a Bic-D–RNP complex and its known functions suggest that it is likely to bind the poly(A) tail or internal mRNA sequences of Bic-D associated RNAs.

Pabp partially colocalizes with Bic-D in the oocyte during mid oogenesis and in blastoderm embryos

We next asked whether Pabp colocalizes with Bic-D in the ovarian germline where *Bic-D* performs different functions. The *pabp–GFP*$^{37\text{-}2}$ gene trap line and anti-Bic-D antibodies, respectively, were used to study Pabp and Bic-D localization during oogenesis, respectively (Fig. 1D). Both are detected in the germline throughout oogenesis and are enriched in the oocyte (Fig. 1D, arrows). Pabp–GFP (green) is first detected in the germarium and it becomes clearly enriched in the oocyte starting at stage 2. From stages 2 to 6, Pabp–GFP (green) is enriched at the posterior cortex of the oocyte, where it partially colocalizes with Bic-D (red) (Fig. 1D, left panels, arrows). In stage 10, Pabp–GFP is primarily expressed in the nurse cells, but it also shows some enrichment at the cortex of the oocyte (Fig. 1D, central panel) and most prominent at the posterior cortex (Fig. 1D, right panel). Homozygous and hemizygous *pabp–GFP*$^{37\text{-}2}$ flies are lethal, indicating that this fusion protein is not entirely functional. We therefore wanted to further confirm the described pattern of Pabp localization by immunostaining wild type ovaries with anti-Pabp antibodies and by staining ovaries that express a myc-tagged Pabp in the germline with anti-myc tag antibodies (*nosGal4:VP16* ≫ *pUASP–myc–pabp–ORF*; Supplementary Figs. S2A-E). Both approaches yielded comparable distribution patterns.

Because Bic-D and Egl are also involved in apical transcript localization in blastoderm embryos (Bullock and Ish-Horowicz, 2001), we also examined the distribution of Pabp in young embryos (Fig. 1E). Similar to Bic-D (red, upper panels), Pabp (green, middle panels) is noticeably enriched apically to the blastoderm nuclei even though a large amount of the protein is also present in the basal cytoplasm (Fig. 1E). Together, the partial co-localization and the biochemical interaction of Pabp with Bic-D are consistent with Pabp being a component of the Bic-D localization machinery.

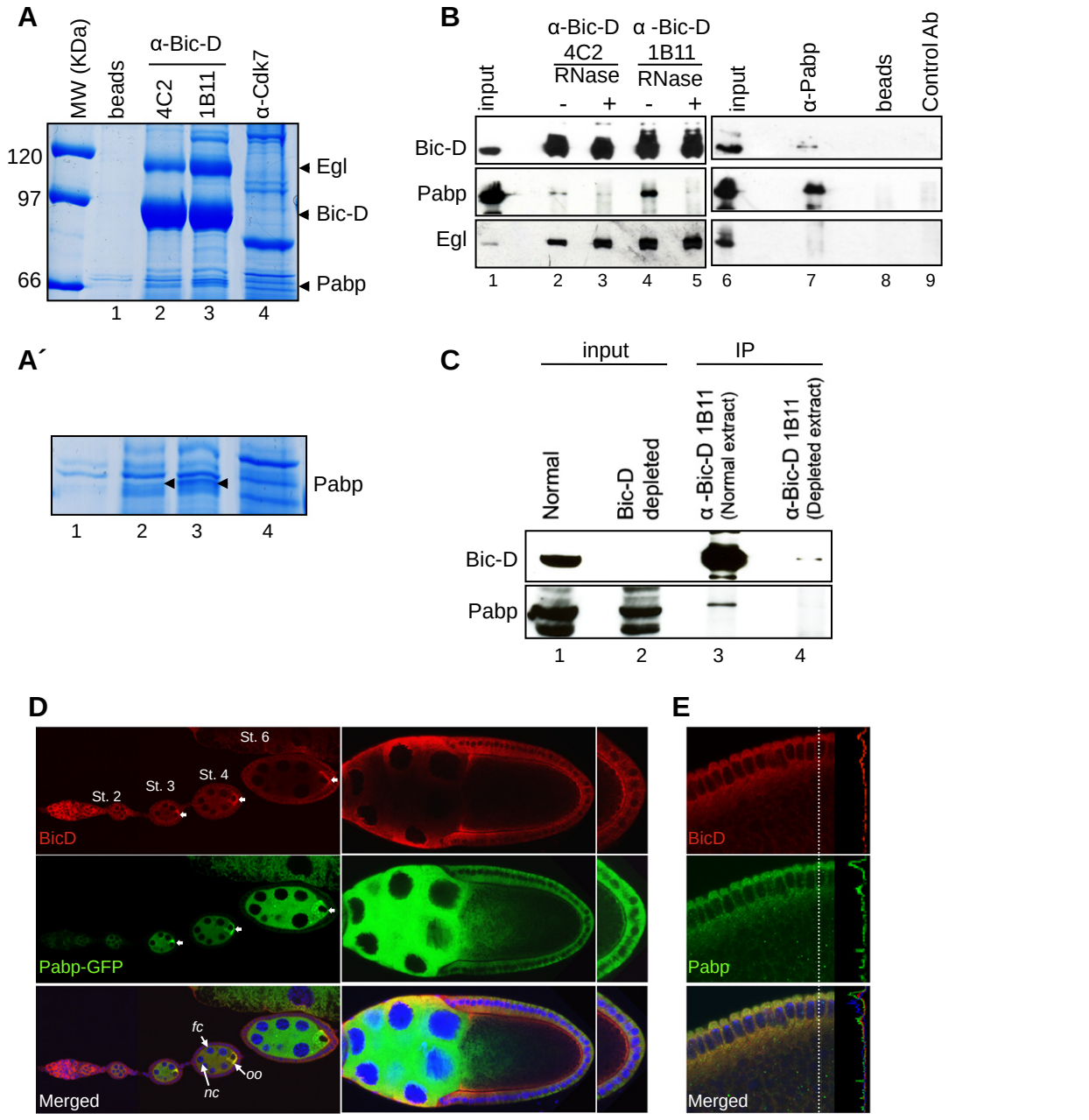

Fig. 1. Pabp associates with Bic-D in an RNA-dependent manner and both proteins partially co-localized in ovaries and young embryos. (A) Immunoprecipitation (IP) of total embryo extracts with anti-Bic-D antibodies 4C2 (lane 2) and 1B11 (lane 3). Anti-Cdk7 antibody (unrelated control protein, lane 4) and protein G beads alone (lane 1) were used as controls for unspecific binding. The IP material was resolved by SDS-PAGE and stained with Coomasie. The gel area containing Pabp, Bic-D and Egl is shown; the bands corresponding to these proteins are indicated by arrowheads. (A′) Magnification of the gel region where Pabp was identified. (B) IP of total embryo extracts with antibodies indicated on top: anti-Bic-D 4C2 (lanes 2 and 3), anti-Bic-D 1B11 (lanes 4 and 5), anti-Pabp (lane 7), beads alone (lane 8) and a control monoclonal antibody against an unrelated murine protein (lane 9). 0.15% of the cytoplasmic extract used for each IP was loaded as input control (lanes 1 and 6). IPs were performed in the presence (+, lanes 3 and 5) or absence (−, lanes 2, 4, 7, 8 and 9) of RNase A. The IP material was resolved by SDS-PAGE, blotted and analyzed by western blot to check for the presence of Bic-D, Pabp and Egl. (C) Normal extract or embryonic extract immunodepleted of Bic-D (with the anti Bic-D 4C2 antibody) were used for IP with anti Bic-D 1B11 antibody. Although Pabp was not immunodepleted (lane 2), it was not precipitated with the 1B11 antibody in the absence of Bic-D (lane 4). (D) Distribution of Pabp and co-localization with Bic-D during oogenesis and early embryogenesis. Immunostaining of phenotypically wild type ovaries (+/*pabp–GFP*$^{37\text{-}2}$) was carried out for Bic-D (red, upper panels) and Pabp-GFP was visualized in the same sample (green, middle panels). Ovaries were counterstained with Hoechst to stain the DNA (blue, in the merged pictures, lower panels). Right panel depicts an enlarged view of the posterior oocyte cortex of the stage 10 egg chamber shown in the central panel. Arrows point to co-localization of Bic-D and Pabp–GFP signals in the oocyte. Oocyte (oo), nurse cells (nc) and follicular cells (fc) are indicated. (E) Immunostainings for Bic-D (red, upper panels) and Pabp (green, middle panels) in syncytial blastoderm embryos. The merged image is shown in the lower panel. Histograms depicted on the right side of the pictures show the fluorescence intensity along the white dotted lines.

pabp is essential during oogenesis

Drosophila pabp is essential for embryogenesis and oogenesis (Clouse et al., 2008; Sigrist et al., 2000b). To address whether Pabp plays a role in the Bic-D dependent transport of mRNAs during oogenesis, we analyzed the gene trap line *pabp–GFP*$^{37\text{-}2}$ and the P-element allele *pabp*^{K10109}, and found that they are zygotic lethal over deficiencies that remove the *pabp* locus. To examine the *pabp*$^{-}$ phenotype in the female germline, we generated germline clones of these lethal alleles using the FLP/FRT *Ovo*^{D} technique (Chou and Perrimon, 1996). The mutant clones supported oocyte formation, but did not develop beyond stages 5–6 (Figs. 2A-B). Under our experimental

conditions, control ovaries from ovo^D females (*FTR G13 ovoD*^{1}/CyO and *ovoD*^{1}*/Dp (?,2) S wg Ms(2)M bw*^{D}) produced only very rarely egg chambers, which then only survived until stages 2–3 of oogenesis. Similarly, in transheterozygous *ovoD*^{1}*/pabp* mutant egg chambers, we observed escapers proceeding only to stage 4 before degenerating. While this already suggests that the observed stages 5–6 egg chambers are indeed *pabp* germline mutants, we still needed to show experimentally that this arrest is caused by the lack of *pabp* activity. We therefore set out to rescue the germline clone phenotypes and the zygotic lethality by introducing a genomic $pabp^+$ copy. Because this indeed rescues these phenotypes (Fig. 2A, right panels), this indicates that most of the egg chambers that reach stages 5–6 represent $pabp^-$ mutant clones that arrest oogenesis because they lack *pabp* activity. Interestingly, by using the FLP–FRT system and a wild type copy of $pabp^+$ on the homologous chromosome, we were unable to observe $pabp^-$ germline clones in adults when inducing them during larval development. Only if induced in the adults we could observe clones at very low frequency (Supplementary Fig. S3). This seems to indicate that $pabp^+$ cells efficiently compete out the $pabp^-$ cells. *pabp* mutant germline clones showed a variety of phenotypes in stages 5–6. These include small oocytes, mispositioned oocytes, packaging defects producing egg chambers with supernumerary nurse cells and two oocytes, polytene nurse cells and multilayered follicle cells (Fig. 2B). Some of these phenotypes may also be due to lack of *pabp* in the follicle cells because recombination was induced through heat shock control and because we observed multilayered follicle cells also in GFP^--marked follicle cell clones (Supplementary Fig. S3). These results show that *pabp* is involved in growth and positioning of the oocyte, in the proper development of nurse cells and follicle cells, and in egg chamber packaging. Interestingly, reduced oocyte growth, abnormal number of germ cells and mispositoned oocytes also result from reduced *Bic-D* activity (Oh and Steward, 2001; Swan and Suter, 1996).

Like Bic-D, pabp is essential for osk mRNA accumulation in the oocyte

The Bic-D/Egl transport machinery is involved in the transport of specific mRNAs including *osk*, *orb, grk* and *Bic-D* mRNAs into the oocyte (Clark et al., 2007; Mach and Lehmann, 1997; Ran et al., 1994; Suter and Steward, 1991). *pabp* mutant germline clones arrest at stages 5–6 of oogenesis (Figs. 2A-B) around the time *osk* RNA null mutants arrest oogenesis (Jenny et al., 2006) and Pabp staining overlaps with *osk* mRNA staining during oogenesis (Supplementary Fig. S2F). Thus, we next asked whether the *pabp* phenotypes could be due to a failure in *osk* mRNA localization to the oocyte. In wild type oogenesis, *osk* mRNA is enriched in the early oocytes and is clearly localized to the posterior compartment by stages 2–3 (Fig. 2C). *osk* mRNA fails to accumulate in this pattern in both *pabp* mutant germline clones (Fig. 2C). In some genetic backgrounds (even in the absence of the FLP chromosome) we also observed that transheterozygous *FRT G13 ovoD*^{1}*/FRT pabp* mutant egg chambers proceeded to stage 4 before degenerating. In contrast to the $pabp^-$ phenotype, these egg chambers showed normal *osk* mRNA accumulation in the oocyte (Fig. 2D). *osk* mRNA showed also oocyte specific accumulation in rarely appearing egg chambers of the genotypes *FRT G13 ovoD*^{1}/CyO and *ovoD*^{1}*/Dp (?,2) S wg Ms(2)M bw*^{D} (Fig. 2D, right panel and data not shown). These results show that *pabp* plays an essential role in the accumulation of *osk* mRNA in the oocyte. Surprisingly, the accumulation of other mRNAs that depend on the Bic-D/Egl transport machinery for their localization was less affected by the *pabp* mutations. In wild type egg chambers, *Bic-D* (Fig. 2E, left panel), *grk* (Fig. 2E right panel), and *orb* (not shown) mRNAs accumulate in the oocyte from stages 2 to 6. Their accumulation in the oocyte was weakly affected (Fig. 2E, lower panels). Some egg chambers show mislocalization of these mRNAs within the oocyte, but these egg chambers also show mispositioning of the oocyte (Fig. 2E, lower panels). This suggests that *pabp* is not directly required for the localization of these mRNAs, but more indirectly through its effect on egg chamber development.

Double *in situs* for *grk* and *osk* mRNA confirmed that in the same *pabp* mutant germline clone only *osk* mRNA accumulation in the oocyte is impaired, while *grk* accumulation is not affected (Fig. 3A). In contrast to the *pabp* germline clone phenotype, mutants that alter egg chamber organization, like for instance DE-cadherin mutants (Godt and Tepass, 1998), cause mislocalization of all 4 mRNAs tested. Lack of *osk* mRNA accumulation in the absence of *pabp* is therefore not an indirect effect of altered over all egg chamber organization, but seems to reflect a more direct transport or stability problem. Using the same confocal microscope settings and different *osk* probes, we observed clear and reproducibly reduced levels of *osk* mRNA signal in *pabp* mutants clones compared to wild type egg chambers (Fig. 3B, left panels). Despite the reduced signal, *osk* mRNA was still detectable in the mutants with enhanced signal detection (Fig. 3B, right panels). These pictures also reveal that *osk* mRNA accumulation in oocytes is reduced in the mutants. While a protocol for quantitative *in situ* hybridization is available (Pare et al., 2009), it does not work to quantify *osk* mRNA levels, presumably because of the presence of multiple *osk* mRNA molecules in each RNP (data not shown). We therefore used a semi-quantitative PCR based approach to assess the effect of *pabp* on *osk* mRNA stability. Compared to *pabp/ovoD* heterozygous egg chambers in the absence of Flipase, the induction of $pabp^{K10109}$ clones using *hs-FLP* causes *osk* mRNA levels to become reduced in samples that contain a mixture of $pabp^{K10109}$*/ovoD* egg chambers and *pabp* germline clones (Figs. 3C, D). In contrast, levels of the control mRNAs *xpd* and *tubulin* were not reduced in these samples. Therefore, *pabp* seems specifically required also to stabilize *osk* mRNA. Interestingly, levels of *osk* mRNA were less affected in $pabp^{GFP37\text{-}2}$ germline clones. These clones still expressed the Pabp–GFP fusion protein, which seems to retain partial *osk* mRNA stabilization function even though it does not facilitate its transport.

Consistently, in wild type ovaries, Staufen accumulates in the oocyte from stage 4 onwards (Fig. 4A, upper panel), a process that depends on *osk* mRNA localization (Jenny et al., 2006). In most of the $pabp^{K10109}$ (Fig. 4A, middle panel) and *pabp–*$GFP^{37\text{-}2}$ (Fig. 4A lower panel) mutants this localization was also abolished. In contrast, Egl (Fig. 4B, left panels) and Bic-D (Fig. 4B, right panels) localization was not affected by the lack of *pabp*. Therefore, *pabp* is specifically required for oocyte accumulation of *osk* mRNA and its binding partner Staufen, but not for the accumulation of other components of the Bic-D localization machinery.

Pabp is a general translation factor that promotes translation by binding to the poly(A) tails of mRNAs (Kahvejian et al., 2005). Mammalian Pabp also represses or enhances translation by binding to A-rich stretches in the 5′ or 3′UTRs of specific mRNAs, including its own (Gorgoni and Gray, 2004; Mangus et al., 2003). Since *osk* mRNA accumulation was severely affected in *pabp* mutants, and because *osk* mRNA is translationally repressed while transported (Wilhelm and Smibert, 2005), we asked whether the lack of Pabp could produce premature translation of *osk* mRNA. Staining with anti-Osk antibodies showed no difference in the Osk expression pattern between wild type and $pabp^{K10109}$ mutant ovaries, indicating that no detectable premature translation took place (Fig. 4C, middle and right panels). However, it needs to be considered that the reduced mRNA levels would also make the detection of Osk protein more difficult.

Reduction of pabp activity suppresses the bicaudal phenotype by reducing anterior mispositioning of osk mRNA

We next studied the genetic interaction between *pabp* and dominant *Bic-D* alleles. Females with the dominant alleles $Bic\text{-}D^{71.34}$ or $Bic\text{-}D^{IIIE48}$ produce embryos with a wide range of patterning defects, including double-abdomen (bicaudal) embryos, which are produced by additional ectopic positioning of *osk* mRNA to the

anterior (Fig. 5A; Ephrussi et al., 1991; Kim-Ha et al., 1991). *Bic-D*$^{71.34}$/*bTft* females produced 16% wild type embryos and 84% embryos with various defects, including reduced mouthparts and bicaudal phenotypes. The mutant phenotypes were suppressed when females carried only one copy of wild type *pabp*$^{+}$ (and either *pabp–GFP*$^{37\text{-}2}$ or *pabp*^{K10109}; Fig. 5B). This interaction was partially reverted by adding

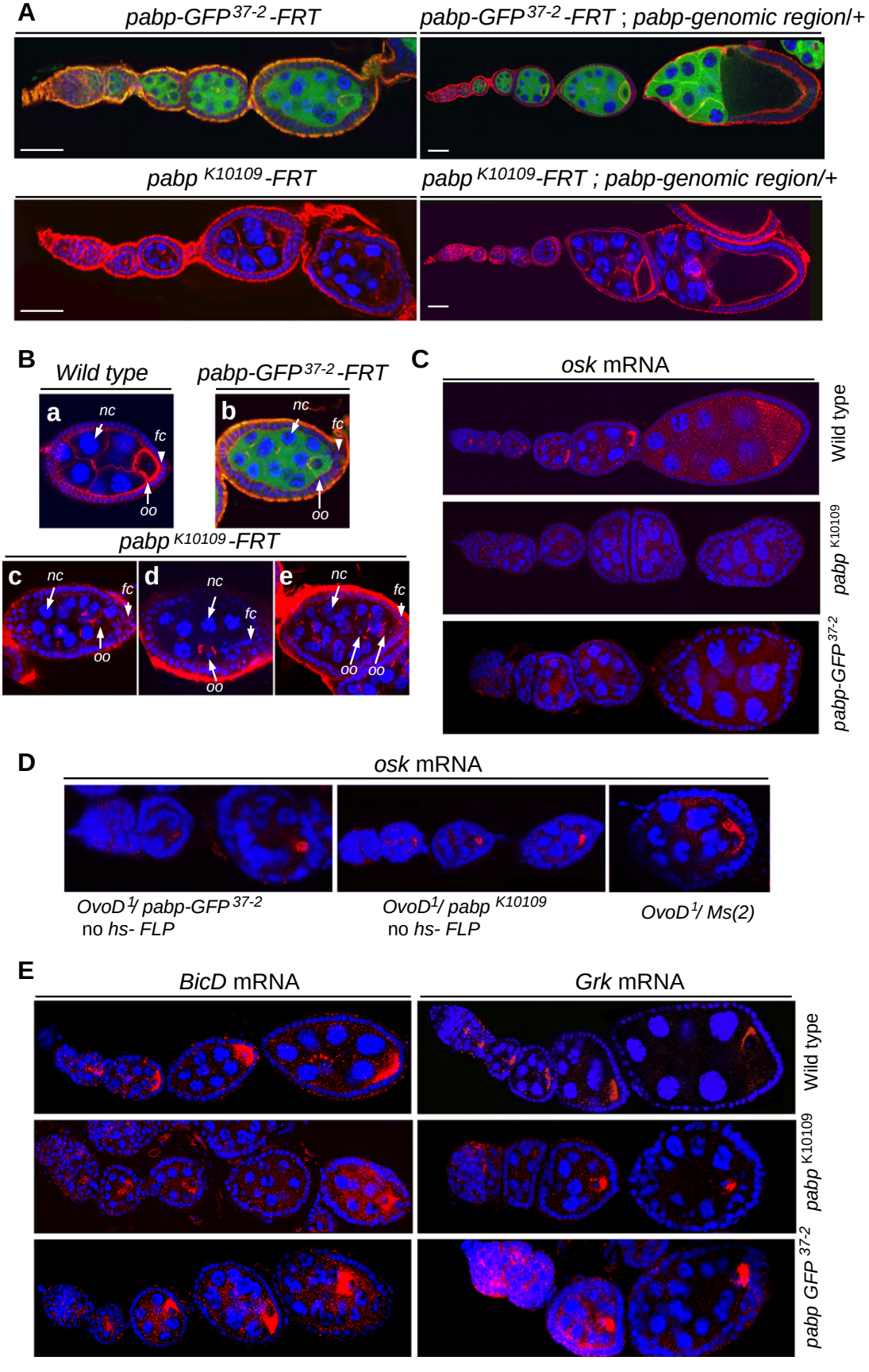

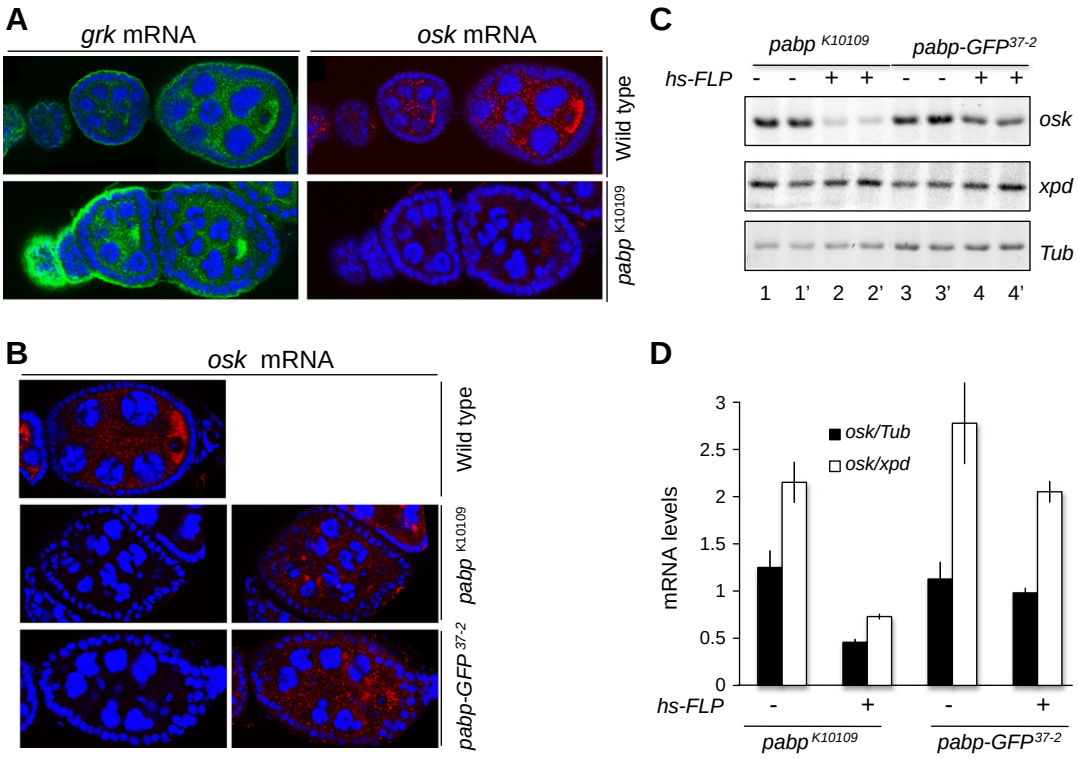

Fig. 3. *pabp* mutant egg chambers show reduced *osk* mRNA levels. (A) *oskar* mRNA accumulation is specifically impaired in *pabp* mutant ovaries. *In situ* hybridization to whole-mount wild type (upper panels) and $pabp^{K10109}$ (lower panels) ovarioles using a mixture of digoxigenin-labeled *grk* (left panels, green) and fluorescein-labeled *osk* (right panels, red) antisense RNA probes showing that *osk* does not properly accumulate in the oocyte in *pabp* mutant egg chambers, while *grk* mRNA localizes properly in the same oocyte. DNA was stained with Hoechst (blue). (B) *in situ* hybridization with *osk* probes in wild type (upper panels) and *pabp* mutant egg chambers (middle and lower panels). The pictures shown on the left where taken with the same settings and show a clear reduction in *osk* mRNA signal in *pabp* mutants. The right panels represent enhanced confocal pictures, showing that *osk* mRNA signal can still be detected in mutant egg chambers despite being much reduced in intensity. (C) Semiquantitative RT-PCR for *osk*, *xpd* and *Tub* mRNAs was performed with RNA prepared from egg chambers of the genotypes $pabp^{K10109}$, *FRT/ovoD, FRT* (lanes 1 and 1′) and $pabp\text{–}GFP^{37\text{-}2}$, *FRT/ovoD, FRT* (lanes 3 and 3′). Flies of the same genetic background, but additionally bearing the heat shock-FLP chromosome were submitted to heat-shock to induce *pabp* germline clones. Ovaries from these flies were used for lanes 2, 2′, 4 and 4′. Under our conditions and 20 PCR cycles using primers that span introns, *osk*, *xpd* and *Tub* mRNA amplifications remained in the exponential range. A representative RT-PCR done in duplicate is shown. (D) The intensity of the *osk* bands from these 2 RT-PCR experiments was quantified with Image J and its abundance was normalized to the unrelated *xpd* and *Tub* mRNAs isolated from the same samples. Samples containing induced $pabp^{K10109}$ germline clones showed reduced levels of *osk* mRNA compared to un-induced samples. Control *xpd* and *Tub* mRNA levels, on the other hand, did not show a reduction upon clone induction. The same results were obtained with 2 independent samples and also when 25 PCR cycles were used for amplification.

a genomic copy of *pabp* (Fig. 5B). Similarly, *pabp* loss-of-function alleles also suppressed the second dominant allele $Bic\text{-}D^{IIIE48}$ (not shown). To find out whether this phenotype correlates with a suppression of anterior mispositioning of *osk* mRNA, we performed RNA *in situ* hybridizations on embryos produced by $Bic\text{-}D^{71.34}$ mothers with two or only one functional copy of $pabp^{+}$ (Figs. 5C-D). Compared to $Bic\text{-}D^{71.34}$/*bTft* mothers, we found an increase in the proportion of embryos showing normal *osk* mRNA localization when the mothers had only one functional *pabp* allele (Fig. 5D). These data show that strong loss-of-function alleles of *pabp* reduce the anterior mislocalization of *osk* mRNA and suppress the bicaudal phenotype.

Pabp–osk interaction: pabp makes osk to become haploinsufficient for embryonic patterning

We next tested for a genetic interaction between *pabp* and *osk*, and found that females transheterozygous for $pabp\text{–}GFP^{37\text{-}2}$ and the *osk* deficiency $Df(3R)pXT^{103}$ produced karyosome fragmentation defects, and oogenesis mostly arrested at stage 7 as in osk^{A87} or $osk^{A187}/Df(3R)pXT^{103}$ females or in *pabp* mutant egg chambers (data not shown; Jenny et al., 2006). This early oogenesis arrest in *pabp–osk* transheterozygous mutants may be caused by reduced *osk* activity. This interpretation is also consistent with another result. Females double heterozygous

Fig. 2. *pabp* is required in the germline and *oskar* mRNA accumulation is specifically impaired in *pabp* mutant germline clones. (A) $pabp\text{–}GFP^{37\text{-}2}$ (upper panels) and $pabp^{K10109}$ (lower panels) mutant egg chambers with or without a *pabp*–genomic rescue transgene were stained with Hoechst to reveal the DNA (blue) and with rhodamine-phalloidine (red) to visualize actin filaments. In $pabp\text{–}GFP^{37\text{-}2}$ and $pabp^{K10109}$ mutant germline clones oogenesis does not proceed further than stages 5–6. Expression of *pabp* from a transgene containing the genomic $pabp^{+}$ region rescues the oogenesis arrest phenotype of both $pabp^{-}$ mutant clones (right panels). (B) (a) Wild type stage 5 egg chamber. (b-e) Examples of the various defects observed in stages 5–6 egg chambers of *pabp* germline mutants. Oocyte (oo), nurse cells (nc) and follicular cells (fc) are indicated. Smaller oocyte, polytene nurse cell nuclei and multilayered follicular cells are observed in *pabp* clones. (d) Egg chamber with mispositioned oocyte. (e) Egg chamber with packaging defects and two oocytes. Oocytes were identified by the presence of 4 ring canals. Scale bars are 30 μm. The presence of slightly older egg chambers in our experiments compared to the one reported by Clouse et al.(2008) may either be caused by differences in the genetic background or growing conditions. Both are known to affect ovary development. (C) *In situ* hybridization to whole-mount wild type ovaries (top), $pabp^{K10109}$ (middle) and $pabp\text{–}GFP^{37\text{-}2}$ (lower panel) mutant germline clones using a digoxigenin-labeled *osk* RNA probe. (D) *osk* mRNA is properly enriched in the oocyte in FRT G13 $ovoD^{1}$/FRT $pabp\text{–}GFP^{37\text{-}2}$ (left panel) and FTR G13 $ovoD^{1}$/FRT $pabp^{K10109}$ chambers (middle panel) (without the hs-FLP chromosome) and FTR G13 $ovoD^{1}$/Dp (?,2) S wg Ms(2)M bw^{D} egg chambers (right panel). (E) *Bic-D* (left panels) and *grk* (right panels) mRNA visualized with antisense RNA probes (red signals).

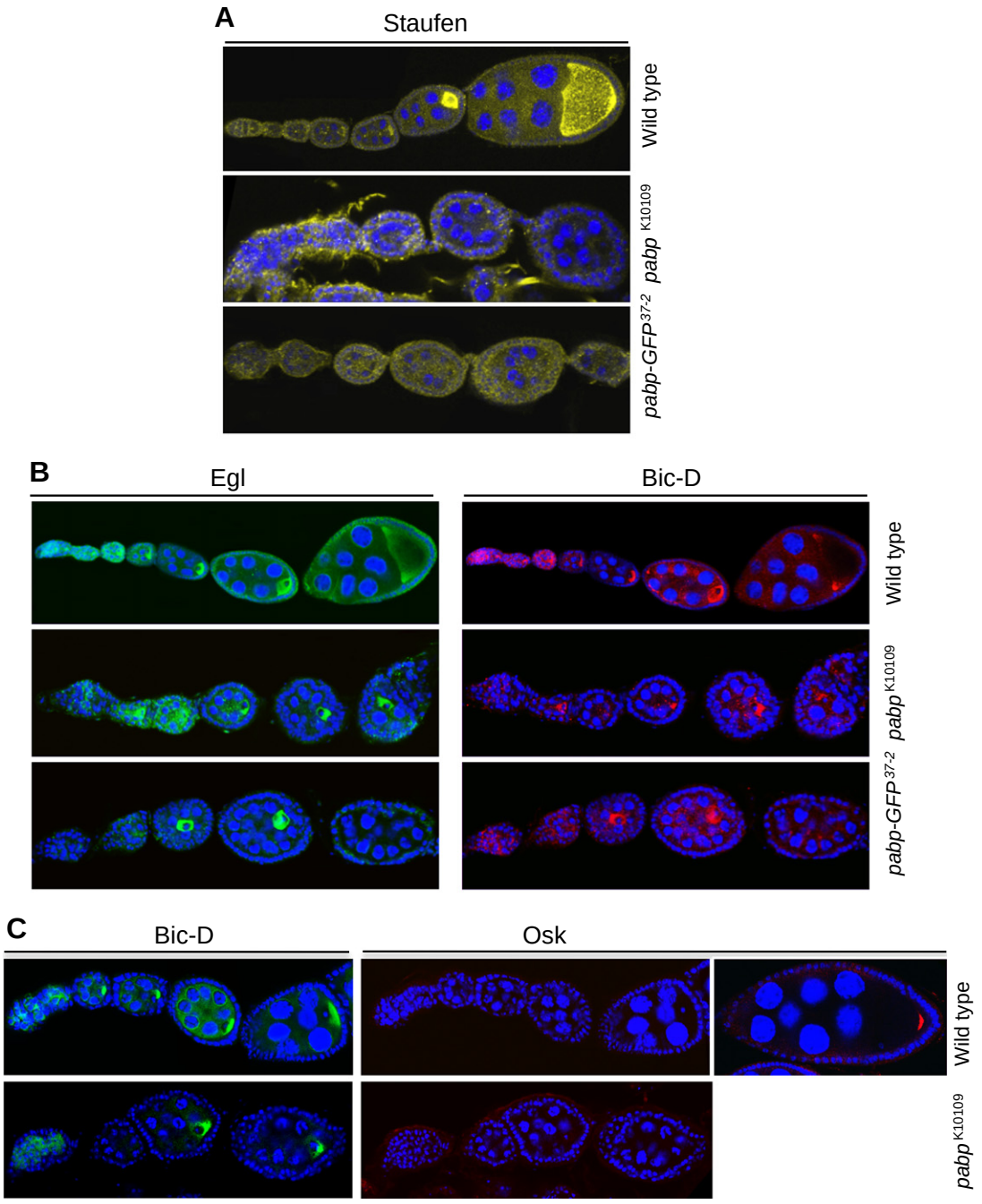

Fig. 4. Stau accumulation in the oocyte is impaired and *osk* is not prematurely translated in *pabp* mutant egg chambers. (A) Wild type (upper panels), $pabp^{K10109}$ (middle panels) and $pabp–GFP^{37\text{-}2}$ (lower panels) ovarioles stained for Stau (yellow) show that Staufen localization requires *pabp*. (B) Wild type (upper panels), $pabp^{K10109}$ (middle panels) and $pabp–GFP^{37\text{-}2}$ (lower panels) egg chambers stained for Egl (left panels, green) and Bic-D (right panels, red). Neither Egl nor Bic-D localization is impaired in *pabp* mutant egg chambers. C) Osk protein is translated only after the *osk* mRNA is anchored at the posterior cortex of stages 9–10 egg chambers of wild type ovaries. Accordingly, no Osk protein signal is observed in younger stages in wild type (upper middle panel). Stage 10 wild type egg chambers, on the other hand, showed Osk protein staining at the posterior of the oocytes in the same preparation, indicating that the staining worked properly (upper right panel). In $pabp^{K10109}$ mutant ovaries *osk* mRNA does not appear to be prematurely translated because the ovarioles showed no Osk staining at all (lower middle panel). Same ovarioles where co-stained for Bic-D (green, left panels), showing accumulation of Bic-D in the oocyte. DNA was also stained with Hoechst (blue).

for $pabp–GFP^{37\text{-}2}$ and either osk^{A87}, osk^{187} or one of three independently generated osk^{-} deficiencies $Df(3R)pXT^{103}$, *Df(3R)BSC506* and $Df(3R)pXT^{26}$ produced much more frequently embryos with strong posterior *osk* phenotypes than females heterozygous for each of these mutations alone (Figs. 5E-F). The *osk* phenotypes in the progeny could be rescued when the mothers had a transgenic copy of the *pabp* genomic region. This indicates that reduced *osk* activity caused by reducing *pabp* and/or *osk* activity itself, is detrimental both for early oogenesis and posterior patterning of the embryo.

Pabp binds A-rich sequences (ARS) in the 3′UTR of osk mRNA

Pabp is expected to generally bind mRNAs through their poly(A) tail and thus to affect them at the same level. However, *pabp* seems to be

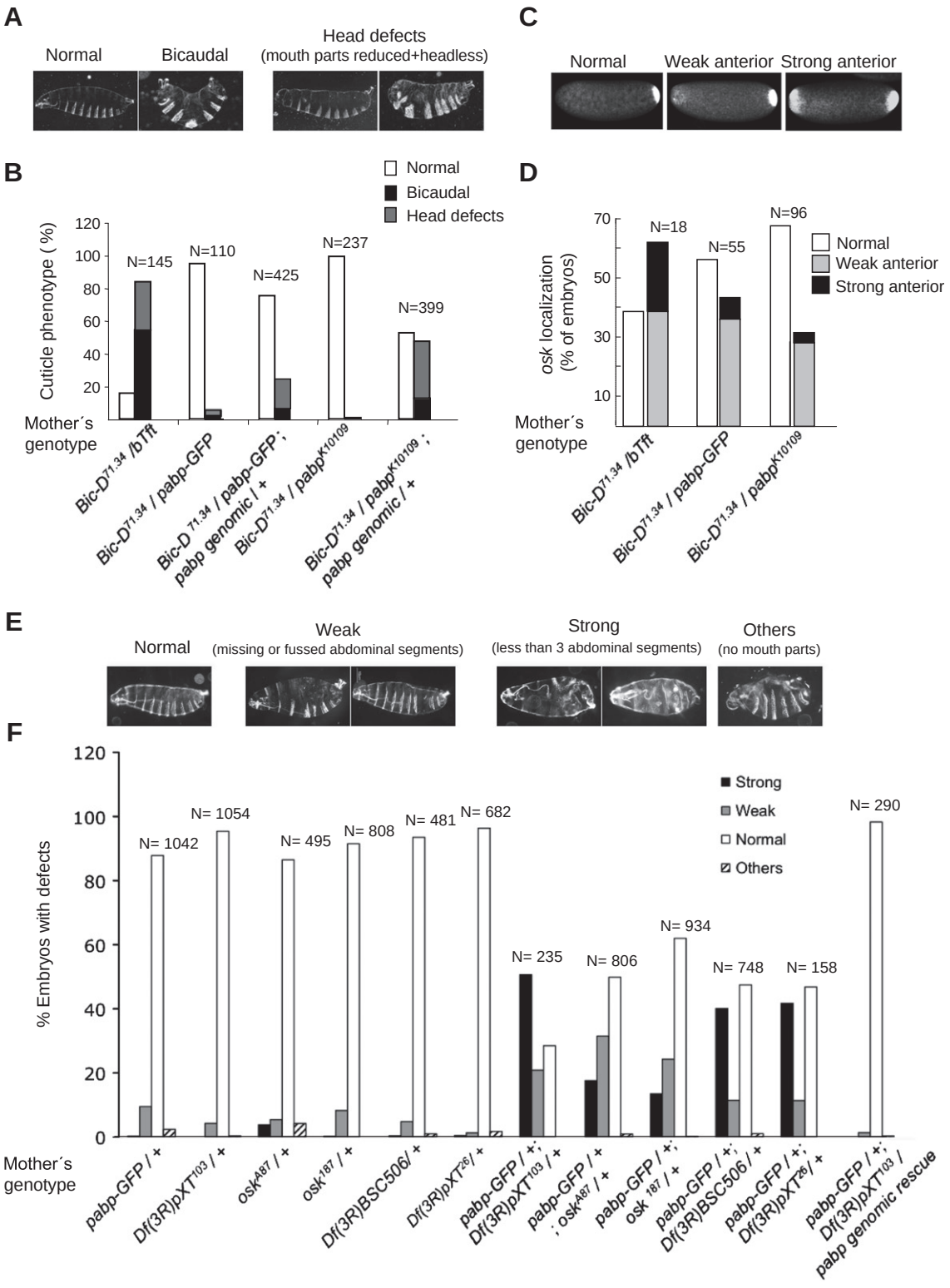

Fig. 5. Genetic interactions between *pabp* and dominant *Bic-D* alleles and *osk* nulls. (A) First instar larval cuticles showing the range of phenotypes associated with the dominant *Bic-D* alleles. (B) Suppression of the bicaudal phenotype in embryos from mothers carrying only one functional allele of *pabp*. The dominant *Bic-D*$^{71.34}$ allele was analyzed for dominant genetic interactions with *pabp*^{K10109} and *pabp–GFP*$^{37\text{-}2}$. Cuticle phenotypes were categorized into three groups for quantification: normal (white bars), head defects (including mouth parts reduced and headless embryos, grey bars) and bicaudals (including symmetric and asymmetric bicaudal embryos, black bars). Results of one set of experiments performed in parallel and under identical conditions for the different genotypes are shown. Qualitatively the same results were obtained in two independent experiments. (C-D) Suppression of *osk* mRNA mislocalization by reducing the *pabp* dose. The dominant allele *Bic-D*$^{71.34}$ was analyzed for its genetic interaction with the *pabp*^{K10109} and *pabp–GFP*$^{37\text{-}2}$ mutants. (C) Embryos showing examples of the different *oskar* mRNA distribution patterns observed. The phenotypes were divided into the three categories shown, allowing us to quantify the phenotypes (D). (E-F) Enhancement of *osk* posterior defects by reduction of *pabp*. The *osk* null alleles *osk*^{A87}, *osk*^{187}, *Df(3R)pXT*^{103}, *Df(3R)BSC506* and *Df(3R)pXT*^{26} were tested for genetic interaction with the *pabp–GFP*$^{37\text{-}2}$ allele. Observed phenotypes were divided into the four categories shown in (E) and the quantified results are shown in (F): normal embryos, weak posterior defects (including embryos with fused or a reduced number of abdominal segments), strong posterior defects (embryos showing less than three abdominal segments) and other defects (mainly embryos showing also anterior defects). + indicates the presence of a wild type chromosome for *pabp* and/or *osk*.

additionally required specifically for the accumulation and stability of *osk* mRNA. Our results raised the intriguing question whether and how Pabp specifically affects this aspect of *osk* mRNA metabolism. It was shown that Pabp can also control translation initiation by binding to A-rich sequences (ARS) consisting of several tracts of 3–8 adenines, present either in the 3′ UTR of the YB-1 mRNA, or in the 5′UTR of its own mRNA and of mRNAs involved in starvation response (Bag, 2001; Gilbert et al., 2007; Patel et al., 2005; Skabkina et al., 2003). Interestingly, the 3′UTR of *osk* mRNA contains six tracts of 3–10 adenines (Fig. 6A) that might be recognized by Pabp. In contrast, no long adenine-tracts are present in the *grk*, *orb* and *Bic-D* mRNA 3′UTRs, whose accumulation in the oocyte was not much affected in *pabp* mutant germline clones. We performed electromobility shift assays (EMSA) and found that recombinant GST–Pabp binds to radio-labeled sense fragments of the *osk* mRNA 3′UTR that contain the ARS but

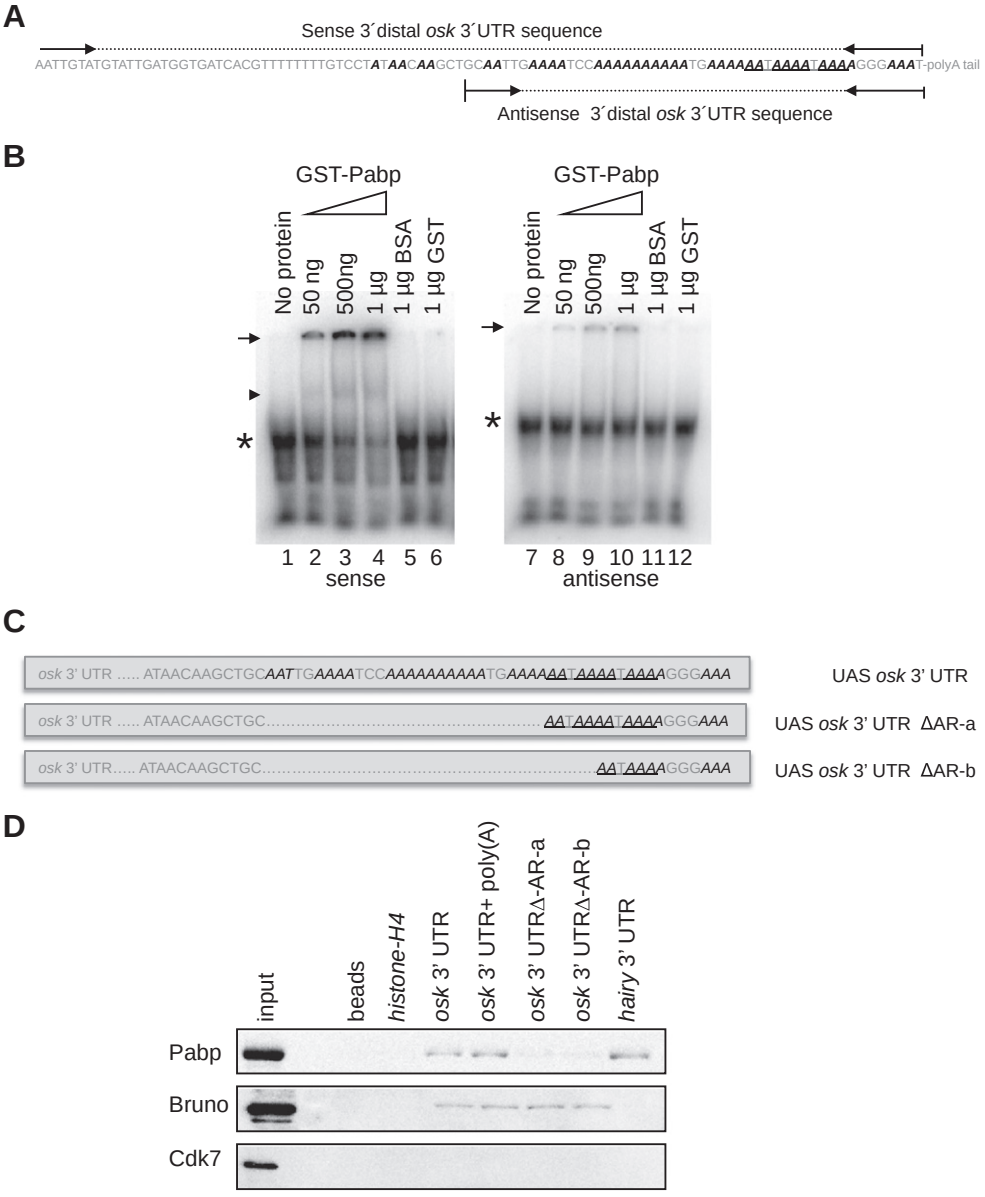

Fig. 6. Pabp binds to an A-rich sequence in the *osk* 3′UTR. (A) Presence of A-rich stretches (italic and bold) in the distal region of the *osk* mRNA 3′UTR. Sense and antisense probes used for EMSA assays are indicated. (B) Band shifting assay using sense (lanes 1–6) and antisense probes (lanes 7–12) (1 pmol, 50,000 cpm) in the presence of increasing concentrations of GST–Pabp (lanes 2–4 and 8–10) or BSA (lanes 5 and 11) or GST (lanes 6 and 12). Lane 1, labeled sense *osk* RNA alone. Lane 7, labeled antisense *osk* RNA alone. The arrow indicates the major high order gel shifted complex. Pabp has been described to form multimers and that is likely the reason why it forms these high molecular weight complexes, which still retain the ability to bind RNA. A faster migrating gel-shifted complex is also observed in the presence of sense *osk* RNA and Pabp (arrowhead). Asterisk shows the migration of free RNAs. Even if there is traces of unspecific binding of the *osk* antisense probe to GST–Pabp, the ratios of RNA in complex with Pabp to free RNA was much higher for the *osk* sense probe. Note also that the amount of free sense RNA was reduced by increasing the amount of GST–Pabp, while free antisense RNA remained almost constant (see asterisks) and no formation of lower order complex is observed. Both complexes can be competed by poly(A) and cold sense probe (Supplementary Fig. S4D-E), indicating that the low mobility band represents specific high order complexes containing Pabp with the *osk* RNA containing the ARS. (C) Schematic representation of the *osk* 3′UTR constructs used in (D). The AR regions are shown and deletions of the sequences AR-a and AR-b are depicted as dotted lines. Underlined sequences represent the putative polyadenylation signals. (D) RNA–protein complexes formed between different biotin-labeled RNAs and extracts of *Drosophila* embryos were purified and monitored for the presence of Pabp, Bruno and Cdk7 as controls. 2% of the embryo extract used for each pull down was loaded as input control. No RNA (beads only), human *histone-H4*, full length *osk* 3′UTR containing a poly(A) tail of 40 nt, full length *osk* 3′UTR, *osk* 3′UTR deleted for A-rich sequences, ΔAR-a and ΔAR-b and *hairy* 3′UTR were used in the pull down assays. Binding of Pabp, but not Bruno, to *osk* 3′UTR was reduced in the *osk* 3′UTRs deleted for the ARS.

no poly(A) tail (Fig. 6B, lanes 2–4). Binding to this RNA was not observed with BSA (lane 5) or GST alone (lane 6). These results were further confirmed by competition experiments (Supplementary Figs. S4D-E).

To further confirm and map this interaction we also performed biotin pull down assays using embryo extracts and biotinylated RNAs from different parts of the *osk* 3′UTR. The *osk* ARS overlap with two putative polyadenylation signals (Figs. 6A,C, underlined). To test the functional requirements of the ARS, we made deletions of the ARS and left intact either both (ΔAR-a) or only one (ΔAR-b) of these predicted polyadenylation signals (Fig. 6C). Biotin labeled full-length *osk* 3′UTRs with or without a poly(A)$_{40}$ tail were able to pull down endogenous Pabp and this binding was considerably reduced when the ARS sequences in *osk* 3′UTR were deleted (Fig. 6D). Interestingly, Pabp was also pulled down with *hairy* 3′UTR, which also contains an A-rich region, but not with a human *histone* RNA, that does not contain A-rich regions (Fig. 6D). In contrast, the binding of Bruno, which binds the Bruno Response Elements (BRE) in a different part of the *osk* 3′ UTR (Kim-Ha et al., 1995), was not affected by deletions in the *osk* A-rich sequences. Bruno did also not bind to *histone* or *hairy* RNAs, which do not contain BREs (Fig. 6D). *histone* and *hairy* RNAs do, however, bind IMP, an RNA binding protein for which they do contain predicted binding sites (data not shown).

In vitro polyadenylation requires an energy source and is inhibited in the presence of Tris buffers like the one used for the biotin pull down assays. It is therefore very unlikely that the binding of Pabp to *osk* mRNA is due to binding to newly added poly(A) tails during the pull down reaction. Despite this, we tested the ability of a known polyadenylation substrate, the *Toll* mRNA (Coll et al., 2010), to become polyadenylated under our conditions. As expected, in our pull down extracts *Toll* mRNAs were not detectably polyadenylated, even though they could be polyadenylated in a normal *in vitro* polyadenylation assay (Supplementary Fig. S5). Similarly, *osk* 3′UTRs were also not polyadenylated under our pull down conditions (Supplementary Fig. S5). Altogether, these results allow us to conclude that Pabp is able to bind the *osk* 3′UTR in a poly(A) tail-independent, but ARS-dependent, manner.

The ARS in the osk 3′UTR are required in vivo for its early oogenesis function

The fact that Pabp can bind *osk* 3′UTRs independent of the poly(A) tail prompted us to study whether the ARS in *osk* 3′UTRs are needed for the early function of *osk* RNA in oogenesis. Till now, no specific sequences in the *osk* 3′UTR have been shown to have this function. $osk^{A87}/Df(3R)pXT^{103}$ females fail to lay eggs and are sterile owing to the early arrest of oogenesis (Jenny et al., 2006). Expression of the *osk* 3′UTR alone from an UAS *osk* 3′UTR transgene driven by a combination of *matα4-GAL4–VP16* and *nos-Gal4–Vp16* is sufficient to rescue the early oogenesis arrest and egg-less phenotype of $osk^{A87}/Df(3R)pXT^{103}$ females and it leads to a normal enrichment of the *osk* 3′UTR RNA in the oocyte in early to mid oogenesis (Figs. 7A-C; see also Jenny et al., 2006). However, as opposed to *osk* mRNA, *osk* 3′UTR RNA fails to localize to the posterior during late oogenesis, as previously described (Figs. 7B-C, right panels; Jenny et al., 2006). To test the function of the ARS during early oogenesis we designed constructs that lack parts of the AR region, but retain both (ΔAR-a) or only one (ΔAR-b) of the predicted polyadenylation signals (Fig. 6C). As opposed to the full length *osk 3′UTR* the expression of the *osk* 3′UTRs lacking AR regions failed to rescue the egg-less phenotype of $osk^{A87}/Df(3R)pXT^{103}$ females (Fig. 7A) and egg chambers did not develop beyond stage 7, even though both transgenic constructs were expressed (Figs. 7C-E). However, the expression levels of both rescue constructs with deletions in the ARS (ΔAR-a and ΔAR-b) were reduced compared with the *osk* 3′UTR wild type rescue construct (Fig. 7F). This result is consistent with a role for Pabp and Pabp binding sites in stabilization of *osk* mRNA. In summary, because both *osk* 3′UTRs lacking AR regions are unable to rescue the egg-less phenotype of $osk^{A87}/Df(3R)pXT^{103}$ mutants (despite becoming at least partially localized to the oocyte in early and middle oogenesis), it is clear that the ARS are essential for the early function of *osk* 3′UTR during oogenesis.

Discussion

Bic-D is involved in transporting diverse cargos including mRNAs, lipid droplets, nuclei and Golgi vesicles, and somehow it also seems to regulate endocytosis (Claußen and Suter, 2005; Larsen et al., 2008; Li et al., 2010; Swift et al., 2010). The transport of these different cargos requires the association of Bic-D with different accessory proteins. In the case of RNA transport, this machinery may also recruit proteins involved in the assembly, translation control and stability of the transported mRNAs. Indeed we identified Pabp, a general translation factor, in RNP complexes containing Bic-D. Pabp seems to be linked to Bic-D through binding to associated RNAs. However, the dynamic participation of Bic-D and Pabp in various different cellular processes and complexes implies that only a fraction of both polypeptides will associate with each other at a given time. This is consistent with the results of our immunoprecipitation experiments, where the Pabp band is much weaker than Bic-D or the band of the general Bic-D–RNA adaptor Egl (Fig. 1). Furthermore, only a fraction of Pabp is precipitated with anti Bic-D anitbodies. However, the RNA-dependent physical interaction, the partial co-localization between Bic-D and Pabp and their genetic interactions point to a role of Pabp in RNA metabolism during the transport process by binding to RNAs associated with Bic-D.

Here we show that Pabp plays a specific role in the proper accumulation in the oocyte of an mRNA that also depends on Bic-D for its localization. *pabp* is required for *osk* mRNA accumulation in the oocyte and for the stability of this mRNA. This conclusion is based on several results that suggest an interaction between these two genes. First, in *pabp* mutant ovaries, accumulation of *osk* mRNA into the oocyte is virtually abolished during early and mid oogenesis, while accumulation of other localized mRNAs is more indirectly affected. The effect on *osk* mRNA accumulation seems to be a combination of reduced levels of *osk* mRNA in mutant egg chambers and lack of localization in the oocyte. Second, *pabp* and *osk* RNA null mutants show similar early oogenesis arrest phenotypes, further suggesting that the two genes act in the same pathway during this stage. Third, the absence of one $pabp^{+}$ copy causes *osk* to become haplo-insufficient, indicating again that the two genes act in the same pathway. Fourth, Pabp binds the ARS in the 3′UTR of the *osk* mRNA and these sequences are essential *in vivo* for early oogenesis to proceed.

The finding that *pabp* affects the accumulation of *osk* mRNA, but not other mRNAs that are localized to the oocyte through Bic-D, is surprising and novel because Pabp is a general factor expected to bind to all mRNAs through their poly(A) tail. Indeed, Pabp is a versatile protein that plays different roles in RNA metabolism. Pabp controls the poly(A) length and stability of mRNAs (Mangus et al., 2003), it participates in nonsense-mediated decay (NMD) (Behm-Ansmant et al., 2007), and it acts as a coactivator of the miRNA-silencing complex (Burgess and Gray, 2010). Aside from this it is also a crucial factor in protein synthesis (Kahvejian et al., 2005; Pestova et al., 2007). During protein synthesis, Pabp interacts with both the eIF4F complex bound to the cap at the 5′ end of the mRNA and with the 3′ poly(A) tail, promoting circularization of the mRNA, allowing the recycling of terminating ribosome's (close-loop-model; Kahvejian et al., 2005; Pestova et al., 2007). However, increasing evidence suggests that the Pabp function in translation is more complex than first recognized and that it goes far beyond its canonical role in the recognition of the poly (A) tails. To date, only few examples show that Pabp can regulate the translation of specific mRNAs (Burgess and Gray, 2010). Stimulation of translation of specific mRNAs takes place by recruitment of Pabp directly to the 3′UTR of the mRNAs as was observed in the case of

A

Female genotype			Total eggs per day			N. females
			Day 1	Day 2	Day 3	
UAS *osk* 3' UTR / Maternal tubulin Gal4	;	nosGal4, *osk* A^{87} / Df(3R) pXT^{103}	165	112	34	28
UAS *osk* 3' UTR ΔAR-a / Maternal tubulin Gal4	;	nosGal4, *osk* A^{87} / Df(3R) pXT^{103}	0	0	0	23
UAS *osk* 3' UTR ΔAR-b / Maternal tubulin Gal4	;	nosGal4, *osk* A^{87} / Df(3R) pXT^{103}	0	0	0	21

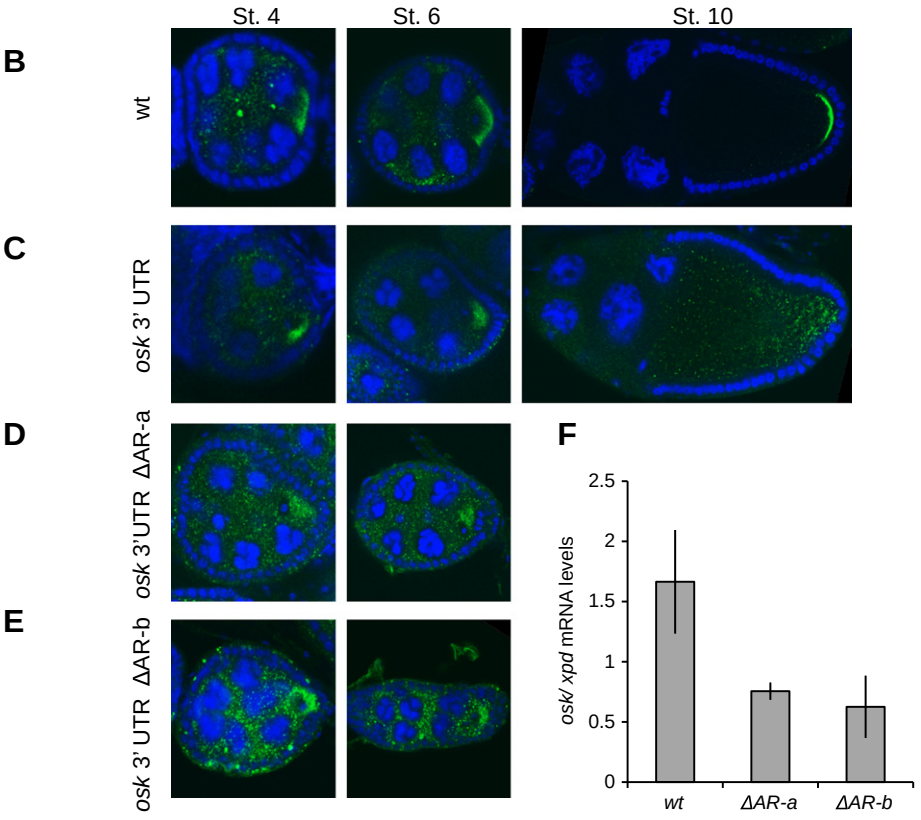

Fig. 7. Pabp binding sequences in the *osk* 3′UTR are required *in vivo* for the early oogenesis function of *osk* RNA. *osk* 3′UTRs deleted for parts of the ARS are not sufficient to rescue the oogenesis arrest phenotype of *osk* RNA null alleles. Full length *osk* 3′UTR plus 1 kb of downstream sequences were used. ARS and the two different deletions of this region, ΔAR-a and ΔAR-b, are depicted in Fig. 6C. (A) Total number of eggs produced per day by the indicated numbers of females (N) of the indicated genotypes. Only the wild type *osk* 3′UTR was able to rescue the egg-less phenotype of the $osk^{A87}/Df(3R)pXT^{103}$ females. Flies were grown at 25 °C, but growing them at 29 °C, where Gal4-induced expression is maximal, gave qualitatively identical results. *In situ* hybridization to whole-mount wild type (B), and $osk^{A87}/Df(3R)pXT^{103}$ egg chambers expressing UAS-driven *osk* 3′UTR (C), *osk* 3′UTR ΔAR-a (D) and *osk* 3′UTR ΔAR-b (E) with an *osk* 3′UTR RNA probe. Note that no older egg chambers are produced when AR sequences are missing from the *osk* 3′UTR. (F) Total RNA from the egg chambers depicted in C-E was purified and subject to semi-quantitative RT-PCR using intron spanning primers to amplify *osk* 3′UTR and *xpd* mRNAs. 20 PCR cycles were used for exponential amplification of *osk* and *xpd* mRNAs. Levels of *osk* mRNAs 3′UTR were normalized to *xpd* mRNA levels for each sample. Same results were obtained in two independent samples.

Dengue virus RNA or YB-1 mRNAs, or indirectly by its recruitment through other proteins (like the DASL family of proteins) to the 3′UTR of target mRNAs. Pabp also binds the 5′UTR of its own mRNA as a complex with Unr and IMP-1 and prevents its own translation by blocking scanning by the 43S complex. In *Drosophila*, *pabp* plays a role in facilitating *grk* translation during late oogenesis, but the molecular mechanism controlling the specificity for *grk* mRNA is not completely understood (Clouse et al., 2008). Thus, to date, only these few examples of mRNA-specific regulation by Pabp have been identified and, to our knowledge, we have now identified the first example of a *pabp* function in the stability of a specific mRNA. This is surprising and raises the possibility that mRNA-specific regulation by Pabp represents a widespread strategy in control of mRNA turnover as well.

In the case of *osk*, the components of the general exon junction complex (EJC), eIF4AIII, Mago and Y14, have also been implicated in specifically localizing *osk* mRNA to the posterior during late oogenesis (Hachet and Ephrussi, 2001; Mohr et al., 2001c; Newmark and Boswell, 1994; Palacios et al., 2004). In this case, it also remains unknown why a general complex can affect specifically the localization of *osk* mRNA and not all mRNAs decorated with the EJC. The

specificity for *osk* mRNA localization might be mediated at least in part through the recruitment of the cytoplasmic protein Btz, which is also needed for posterior *osk* localization, by eIF4AIII. This complex would then recruit the cytoplasmic localization factors to the correctly spliced and exported transcripts (Hachet and Ephrussi, 2001; van Eeden et al., 2001). Similarly to the EJC, Pabp may recruit other proteins specifically to *osk* mRNA, and these proteins may then be involved in mediating mRNA stability or repressing RNA degradation. The recent finding that mammalian Pabp can bind to microtubules (Chernov et al., 2008) also hints that Pabp may help linking *osk* mRNA to the transport machinery in addition to controlling its RNA stability. Indeed, *in situ* staining experiments showed that the remaining *osk* mRNA in the *pabp* mutant is also less efficiently localized to the oocyte (Fig. 3B). Consistent also with a role for Pabp in the RNA transport manchinery is the fact that Pabp was also shown to bind, in concert with other proteins, to sequences in the *bicoid* and *Vasopresin* mRNAs, which are essential for correct localization of these transcripts in oocytes and dendrites, respectively (Arn et al., 2003; Mohr et al., 2001a, 2001b; Mohr and Richter, 2004). Pabp is also needed for maintaining the localization of Ash1 mRNA to the bud tip in yeast (Trautwein et al., 2004). However in this case the exact mechanism by which Pabp is regulating specifically these mRNAs is not known.

Thus, given the immense number of interaction partners of Pabp, there is plenty of potential for Pabp to regulate in a similar manner additional specific RNAs at the level of stability, localization, translation, storage and anchoring. Interestingly, weak alleles of *pabp* display a male meiotic phenotype with defects in spindle formation, chromosome segregation and cytokinesis (Blagden et al., 2009). These findings also point to a role of *pabp* in regulating specific genes during many different and essential cellular processes.

The fact that lack of Pabp reduces *osk* mRNA levels, points to the question of how Pabp can regulate the stability of *osk* mRNA. Interestingly, the nuclear poly(A)-binding protein, Pabp2, has been shown to act in conjunction with Ccr4 to shorten the poly(A) tail of specific mRNAs including *osk* and, in yeast, deadenylation by Ccr4 is inhibited *in vitro* by cytoplasmic Pabp (Benoit et al., 2005; Tucker et al., 2002). On the other hand, there is evidence that Pabp and Pabp2 can coexist on the same poly(A) tails. This could suggest that in the absence of Pabp, Pabp2 may be recruited preferentially to *osk* mRNA through the same ARS, the *osk* 3′UTR or even through the poly(A) tail, promoting its deadenylation and thus is degradation. Preliminary results suggest that Pabp2 is also able to bind *osk* 3′UTR, although its binding was not reduced in ΔARS deletion mutants or in the absence of the poly(A) tail (not shown). This is not surprising since yeast Pabp2 is also able to bind cotranscriptionally to most mRNAs even before the poly(A) tail is synthesized and it remains associated with the mRNAs during translation (Lemieux and Bachand, 2009). Thus, in *pabp* mutants, the recruitment of Pabp2/Ccr4 could be favored, compromising the stability of *osk* mRNA. Recent evidence also indicates that yeast Pabp2 binds directly to the exosome, a complex containing multiple 3′−>5′ exonucleases, and that this interaction is required for the maturation of snoRNAs (Lemay et al., 2010; Libri, 2010). An attractive idea is that in the case of *osk* mRNA the direct binding of Pabp to the distal region of its 3′UTR, very closed to the poly (A) tail, could favor the association of more Pabp molecules (through their multimerization domains; Melo et al., 2003) and dissociation of Pabp2 from newly synthesized mRNAs, thus favoring mRNA stability and dissociation from the Ccr4 deadenylase or exosome complex. Interestingly, the *Drosophila* decapping protein 1 (dDcp1) is also a component of the *osk* mRNP and required for *osk* mRNA transport. However, although dDcp-1 is associated with *osk* mRNA during oogenesis, it seems that it does not initiate mRNA decay since *osk* mRNA degradation is repressed until embryogenesis (Lin et al., 2006). The role of Pabp in inhibiting decapping is well established in other situations (Parker and Song, 2004). Pabp bound to the *osk* ARS and/or to the poly(A) tail may therefore function to inhibit the decapping activity of *osk*-bound dDcp1 and thus promote stability of *osk* mRNA.

Whatever the mechanism of mRNA degradation that is triggered in the absence of Pabp, *osk* ARS not only function in RNA stability, but they are also essential for oogenesis to proceed through the early stages. Since *osk* RNA is needed for early oogenesis, Jenny and colleagues suggested that *osk* 3′UTR RNA might provide a scaffold function, bringing into the oocyte cytoplasmic factors essential for the progression of oocyte development or sequestering a factor that would otherwise inhibit oogenesis (Jenny et al., 2006). Because Pabp still concentrates in *osk* RNA null oocytes (Supplementary Figs. S4A-C), Pabp itself does not seem to be one of these factors. However, the fact that yeast Pabp binds efficiently eIF4G when Pabp is bound to poly(A) tails (Tarun and Sachs, 1996), suggests the hypothesis that only Pabp in complex with *osk* RNA may be able to recruit such oogenesis factors or to sequester oogenesis inhibiting factors.

Materials and methods

Drosophila stocks

pabp^{K10109}, *Df(2R)Pcl7B*, *Df(PC4)*, *Df(3R)pXT*^{103}, P{matα4-GAL–VP16}, Nos-Gal4:Vp16 stocks were obtained from the Bloomington *Drosophila* Stock Center. *pabp–GFP*$^{37\text{-}2}$ was kindly provided by Alain Debec and *osk*^{A87} and *osk*^{187} by Anne Ephrussi (Jenny et al., 2006). Females homo- or hemizygous for the *pabp* alleles *pabp*^{K10109} and the *pabp–GFP*$^{37\text{-}2}$ are lethal. For germline clonal analysis, a FRT site was recombined onto the *pabp*^{K10109} and *pabp–GFP*$^{37\text{-}2}$ chromosomes. *pabp* germline clones were induced using the FLP/FRT *Ovo*^{D} technique (Chou and Perrimon, 1996). Transgenic flies with genomic *pabp*, UAS-*osk* 3′UTR, UAS-*osk* 3′UTR ΔAR-a and UAS-*osk* 3′UTR ΔAR-b were generated using the germ-line-specific phiC31 integrase transgenesis system (Bischof et al., 2007; Koch et al., 2009). The line *y w*; +; attP-64A was used to generate all transgenic lines. Tests for enhancement of the bicaudal phenotype were done in the absence of the *CyO* balancer (because this would enhance the phenotype) and repeated on different days to control for environmental effects (Mohler and Wieschaus, 1986).

DNA constructs

The Bac clone RP-98-33K9 containing the *pabp* gene (Bac Resourses, Oakland Research Institute, U.S.A.) was cut with Apa I, BamHI, SacII and EcoRV. A 7.8 kb fragment containing the *pabp* gene plus 1 kb downstream and 1.3 kb upstream sequences was cloned as an ApaI–EcoRV fragment into pBluescript, and further subcloned as a KpnI–NotI fragment into pCaSpeR–AttB to create the plasmid pCaSperR–AttB–*pabp* genomic. The genomic *osk* fragment consisting of the entire *osk* 3′UTR and about 1 kb of the 3′ flanking sequences was described to rescue the *osk* RNA null egg less phenotype by Jenny et al. (2006). This fragment was amplified by PCR from a λ genomic library and cloned into the pCRII-Topo vector to generate the plasmid *osk* 3′UTR genomic-PCRII-Topo. PCR mutagenesis using primers with flanking BglII and BamHI restriction sites and *osk* 3′UTR genomic-PCRII-Topo vector as template were used to produce the corresponding deletions of the ARS in the *osk* 3′UTR in order to generate the plasmids *osk* 3′UTR genomic ΔAR-a-PCRII-Topo and *osk* 3′UTR genomic ΔAR-b-PCRII-Topo. The insert from these plasmids were liberated with BglII/BamHI and ligated into the BamHI site of the pUASP–K10–AttB vector to generate the transgenic vectors UAS–*osk* 3′UTR, UAS–*osk* 3′UTR-ΔAR-a and UAS–*osk* 3′UTR-ΔAR-b, respectively. A BamHI–XbaI 6x myc-tag fragment was inserted into the BglII/XbaI site of pUASP–K10–AttB to generate pUASP–myc–K10–AttB. The Open Reading Frame (ORF) of *pabp* (Roy et al., 2004) was cloned into the XbaI site of pUASP–myc–K10–AttB to generate the construct

pUASP–myc–pabp ORF–K10–AttB. This construct was used to generate the myc-tag-*pabp* transgen.

Immunoprecipitations (IPs), mass spectrometry and western blots

Due to cross reactivity of the 1B11 antibody with Translin, total extracts from *translin*^{null} mutant embryos that show no visible phenotype were used as starting material (Claußen et al., 2006). One gram of dechorionated 0–8 h old embryos was homogenized on ice in 2 ml of homogenization buffer (HB; 25 mM Hepes pH 7.4, 150 mM NaCl, 0.5 mM EDTA, 1 mM DTT, and EDTA-free protease inhibitor cocktail Complete TM; Roche Diagnostics). The supernatant was centrifuged twice at 16,000 ×*g* for 40 min at 4 °C. For mass spectrometry analysis, 4 ml of 1B11, 8 ml of 4 C2 or 4 ml of Cdk7 monoclonal antibody supernatant were incubated with 80 µl of protein-G Sepharose beads (Amersham) for 1 h at room temperature. After extensive washing with PBS, the bead-antibody complexes were incubated at 4 °C overnight on a wheel with 4 ml of embryo extract per IP. The unbound material was washed off 7 times with HB. Beads were allowed to settle by gravity between washes and were transferred to new tubes in the first and last washes. The IP material was resuspended in 40 µl of sample buffer and resolved by SDS-PAGE. Proteins were stained with Coomassie Brillant Blue (Invitrogen). Visible bands were cut and in-gel digested with trypsin. Eluted peptides were sequenced by liquid chromatography-coupled ESI tandem MS (LC-MS/MS) on a Q-ToF Ultima instrument (Waters) as described (Bessonov et al., 2008). Proteins were identified by searching fragment spectra against NCBInr database using MASCOT (Matrix Science, London) as a search engine, and confirmed by cross search in the *Drosophila* database FlyBase (flybase.org). For western blot analysis, IPs using 30–40 µl beads and 1 ml of embryo extracts were performed. Embryos were homogenized in homogenization buffer containing magnesium ($MgCl_2$–HB; 25 mM Hepes pH 7.4, 50 mM KCl, 1 mM DTT, 1 mM $MgCl_2$ and EDTA-free protease inhibitor cocktail). For monoclonal antibodies against Bic-D, GFP and the murine control antibody, 1 ml of antibody supernatant was used per IP. For polyclonal anti-Pabp antibodies (Roy et al., 2004) 2 µl of antibody were diluted in 1 ml of PBS. When present, RNase A was added to a final concentration of 0.35 mg/ml right after mixing the antibody-bead complexes with the embryo extracts. The beads were resuspended in 30 µl of sample buffer and 7.5 to 15 µl per well was analyzed. Western blots were performed using the rabbit anti-Pabp (1:5000 dilution; Roy et al., 2004), anti-Egl (1:5000; Mach and Lehmann, 1997), anti-Bruno (1:3000, gift from Mary Lilly) and mouse anti-Bic-D (a mix of 1B11 and 4C2, 1:10 dilution; Suter and Steward, 1991) antibodies, and horseradish peroxidase-conjugated secondary antibodies (GE Helthcare).

Immunostainings

Immunostainings of whole-mount ovaries and embryos were done using the following primary antibodies: mouse anti-Bic-D (a mix of 1B11 and 4C2, 1:10 dilution), rabbit anti-Pabp (1:2500 dilution; Roy et al., 2004) or rabbit anti-Pabp (1:100 dilution; Sigrist et al., 2000a), rabbit anti-Osk (1:500 final dilution; Markussen et al., 1995), rabbit anti-Egl (1:5000 final dilution; Mach and Lehmann, 1997), rabbit anti-Staufen (1:2000 dilution; St Johnston et al., 1991), and anti-myc 9E10 (Developmental Studies Hybridoma Bank; dilution 1:5). Secondary antibodies were Cy3-conjugated anti-mouse, Cy5-conjugated anti-rabbit (Jackson Immunoresearch), A495 anti-rabbit and OregonGreen 488 anti-mouse (Molecular Probes). Where required, nuclei and actin filaments were stained for 20 min with 2.5 µg/ml Hoechst 33258 and 1 unit/ml rhodamine-conjugated phalloidin (Molecular Probes), respectively, during the final washing steps. Images were analyzed with a Leica TCS-SP2 confocal microscope.

In situ hybridization to whole mount embryos and ovaries

Linearized pBS–*oskar*, the EST LD32255 (BDGP resources) containing the *grk* cDNA, pBS–*Orb* E4 cDNA (Lantz et al., 1992) and Bic-D-short-pBSK were used as templates to generate digoxigenin-labeled RNA antisense probes. *In situ* hybridization experiments were performed as described (Hughes and Krause, 1999) with the following modifications. Ovaries were dissected in Ringer's solution and fixed in a mixture of 200 µl of 4% Paraformaldehyde in PBS, 600 µl Heptane and 20 µl of DMSO for 20 min on a wheel. Ovaries were washed three times for 10 min in PBT (PBS, 0.1% Tween) and then treated with proteinase K (50 µg/µl) for 2 min. The ovaries were blocked in MAB-blocking buffer (1X Maleic acid buffer (MAB) (500 mM Maleic acid, 750 mM NaCl, pH 7.5) containing 20% donkey serum (Chemicon), 2% Roche blocking reagent and 0.05% Tween-20 and further washed with MABT (MAB plus 0.05% Tween). The digoxigenin-labeled probes were detected with sheep-anti-digoxigenin antibody in MAB-block (Roche) and Cy3-conjugated donkey anti-sheep IgG F(ab′)2 fragments (Jackson Immunoresearch). During the final washing steps the nuclei were stained by adding 2.5 µg/ml of Hoechst 33258 (Molecular Probes). Images were analyzed by confocal microscopy. Double *in situ* hybridization experiments were performed as described (Hughes and Krause, 1999) with the following modifications in the antibodies used. Digoxigenin-labeled probes were detected with sheep-anti-digoxigenin antibody (Roche) and Cy5-conjugated donkey anti-sheep (Jackson Immunoresearch). Fluorescein-labeled probes were detected with mouse anti-fluorescein antibody (Roche) and Cy3-conjugated goat anti-mouse antibody (Jackson Immunoresearch). For *in situ* hybridization combined with protein detection, the same protocol was used, but the proteinase K treatment was omitted.

Electrophoretic mobility shift assay (EMSA)

EMSA were done as described (Schultz et al., 2006). Briefly, 50,000 counts (1 pmol) of ^{32}P-labeled sense or antisense *osk* 3′-UTR distal probes were incubated with different concentrations of recombinant GST–Pabp or BSA (Biolabs) or GST and 10 µg of *Escherichia coli* tRNA (Sigma) for 1 h at 4 °C in a final volume of 15 to 20 µl of buffer B (50 mM Tris–HCl pH 8.0, 150 mM NaCl, 1 mM EDTA, 1 mM DTT, 2% Triton X-100). Subsequently, RNA and RNA–protein complexes were resolved on a 5% (36:1) native polyacrylamide mini-gel containing 0.5× Tris borate-EDTA and visualized with a PhosphorImager. DNA templates to prepare *osk* RNA probes were generated by PCR. *In vitro* transcription was done using T7 RNA polymerase (Stratagene) in the presence or absence of [α-^{32}P]ATP (Amersham), treated with DNase I, extracted with phenol: chloroform, spun through a mini Quick Spin G50 column (Roche) and precipitated with NH_4Ac/EtOH. RNA integrity was checked in a 7 M urea/6% polyacrylamide gel (19:1). For competition assays, recombinant GST–Pabp protein was preincubated with increasing amounts of cold RNAs, poly(A) or poly (G) (Sigma), and 10 µg of *E. coli* tRNA in buffer B for 20 min on ice before it was incubated for 1 h at 4 °C with ^{32}P-labeled sense *osk* 3′ UTR distal probe.

Recombinant protein purification

Fusion proteins were expressed in *E. coli* BL21 (DE3) using the plasmids pGST–dPabp (Roy et al., 2004) and pGEX6P2 (Amersham Pharmacia Biotech). Glutathione S-transferase was purified on Glutathione-Sepharose resin (Amersham Pharmacia Biotech) according to the manufacturer's recommendations. The small soluble fraction of GST–Pabp was purified according to published protocols (Khaleghpour et al., 2001; Roy et al., 2004). Recombinant proteins used for EMSA

assays were dialyzed against 1× PBS (137 mM NaCl, 2.7 mM KCl, 4.3 mM $Na_2HPO_4.7H_2O$, 1.4 mM KH_2PO_4, pH 7.4) containing 1 mM DTT.

Synthesis of biotinylated RNAs and pull-down experiments

DNA templates for biotin-RNA synthesis of the *osk* 3′UTR sequences were prepared by PCR from the plasmids pBS–*osk*, UAS–*osk* 3′UTR-ΔAR-a and UAS–*osk* 3′UTR-ΔAR-b, with a sense primer carrying a T7 RNA polymerase promoter sequence at its 5′-end and the corresponding antisense to generate *osk* 3′UTR + poly(A)$_{40}$, *osk* 3′UTR and *osk* 3′ UTR-ΔAR-a and *osk* 3′UTR-ΔAR-b, respectively. Primers carrying also the T7 polymerase promoter and specific antisense primers were used to generate human *histone-H4* and *hairy* 3′ UTR by PCR using cDNA clones as templates. PCR products were gel purified and served as templates to prepare biotinylated RNAs using the Biotin RNA labeling mix (Roche Diagnostics) and T7 polymerase (Roche Diagnostics). Biotinylated RNAs were treated with RNase-free DNase I and purified using the RNeasy kit (Quiagen). Each biotinylated RNA was analyzed by agarose gel electrophoresis and quantified by UV-spectrometry.

Biotin-RNA-pull-down experiments were performed essentially as described (Gerber et al., 2006). Embryo extracts were prepared by homogenizing 0.2 gr of embryos in 2 ml of extraction buffer (20 mM Tris–HCl pH 8.0, 150 mM NaCl, 0.5 mM EDTA pH 8.0, 5% glycerol, 0.1% Triton-X100, 1 mM DTT, 0.2 mg/ml Heparin, 0.2 mM mg/ml tRNA, 2 mM $MgCl_2$, 1 mg/ml BSA, 20 U/ml DNase I (Roche Diagnostics), 40 U/ml RNase inhibitor (Biolabs), protease inhibitor cocktail; Roche Diagnostics). 10 pmol of biotinylated RNA were mixed with 200 µl extract and incubated on a rotator for 30 min at room temperature. Preequilibrated Streptavidin Paramagnetic Beads (100 µl, Promega) in extraction buffer were added to each binding reaction and the mixture was further incubated for 30 min. Beads were then captured with the magnet, washed 8 times for 10 min at 4 °C with extraction buffer and boiled in 40 µl SDS-sample buffer. 7 µl were resolved on a 10% SDS-protein gel and subjected to immunoblot analysis using anti-Pabp (1:5000), anti-Bruno (1:3000) or anti-CDK7 (1:10) antibodies. To test for polyadenylation activity of the extracts, a *Toll* mRNA was used as substrate and a positive polyadenylation test assay was performed as described (Coll et al., 2010).

RT-PCR assays

RNA from 5 to 10 ovaries was extracted using the RNeasy kit (Quiagen) following the instruction manual. Primers used for the RT-PCR analysis were designed to span introns. Sequences were amplified using the Access RT-PCR system (Promega). 20 to 30 cycles were tested to identify the exponential range of amplification using 200 ng of total RNA, and 20 cycles were identified as ideal for the amplification kit used.

Acknowledgments

We thank H. Imboden, N. Sonenberg, S. Sigrist, A. Ephrussi, P. Lasko, A. Debec, BJ Schnapp, M. Ruepp, M. Lilly, F. Gebauer and R. Lehmann for antibodies, constructs and flies stocks. Our thanks also go to Rafael Koch for the pCaSpeR-AttB and pUASP-K10-AttB vectors, to Jacqueline Adam and Corinne Roesselet for their help with the construction of the pUASP-*myc-pabp* ORF-K10-AttB, to Olivier Urwyler, Simon Bullock and Joel Anne for comments on the manuscript. Michael Altmann, Annemarie Schultz, Fatima Gebauer, Olga Coll and Andre Gerber are acknowledged for their technical advice. We specially thank Greco Hernandez for valuable comments on the manuscript and useful discussions. This work was supported by the Swiss National Science Foundation and the Canton of Bern.

Appendix A. Supplementary data

Supplementary data to this article can be found online at doi:10.1016/j.ydbio.2011.07.009.

References

Arn, E.A., Cha, B.J., Theurkauf, W.E., Macdonald, P.M., 2003. Recognition of a bicoid mRNA localization signal by a protein complex containing Swallow, Nod, and RNA binding proteins. Dev. Cell 4, 41–51.
Bag, J., 2001. Feedback inhibition of poly(A)-binding protein mRNA translation. A possible mechanism of translation arrest by stalled 40 S ribosomal subunits. J. Biol. Chem. 276, 47352–47360.
Behm-Ansmant, I., Gatfield, D., Rehwinkel, J., Hilgers, V., Izaurralde, E., 2007. A conserved role for cytoplasmic poly(A)-binding protein 1 (PABPC1) in nonsense-mediated mRNA decay. EMBO J. 26, 1591–1601.
Benoit, B., Mitou, G., Chartier, A., Temme, C., Zaessinger, S., Wahle, E., Busseau, I., Simonelig, M., 2005. An essential cytoplasmic function for the nuclear poly(A) binding protein, PABP2, in poly(A) tail length control and early development in *Drosophila*. Dev. Cell 9, 511–522.
Besse, F., Ephrussi, A., 2008. Translational control of localized mRNAs: restricting protein synthesis in space and time. Nat. Rev. Mol. Cell. Biol. 9, 971–980.
Bessonov, S., Anokhina, M., Will, C.L., Urlaub, H., Lührmann, R., 2008. Isolation of an active step I spliceosome and composition of its RNP core. Nature 452, 846–850.
Bischof, J., Maeda, R.K., Hediger, M., Karch, F., Basler, K., 2007. An optimized transgenesis system for *Drosophila* using germ-line-specific phiC31 integrases. Proc. Natl. Acad. Sci. U. S. A. 104, 3312–3317.
Blagden, S.P., Gatt, M.K., Archambault, V., Lada, K., Ichihara, K., Lilley, K.S., Inoue, Y.H., Glover, D.M., 2009. *Drosophila* Larp associates with poly(A)-binding protein and is required for male fertility and syncytial embryo development. Dev. Biol. 334, 186–197.
Bullock, S.L., 2007. Translocation of mRNAs by molecular motors: think complex. Semin. Cell Dev. Biol. 18, 194–201.
Bullock, S.L., Ish-Horowicz, D., 2001. Conserved signals and machinery for RNA transport in *Drosophila* oogenesis and embryogenesis. Nature 414, 611–616.
Burgess, H.M., Gray, N.K., 2010. mRNA-specific regulation of translation by poly(A)-binding proteins. Biochem. Soc. Trans. 38, 1517–1522.
Chernov, K.G., Curmi, P.A., Hamon, L., Mechulam, A., Ovchinnikov, L.P., Pastre, D., 2008. Atomic force microscopy reveals binding of mRNA to microtubules mediated by two major mRNP proteins YB-1 and PABP. FEBS Lett. 582, 2875–2881.
Chou, T.B., Perrimon, N., 1996. The autosomal FLP–DFS technique for generating germline mosaics in *Drosophila melanogaster*. Genetics 144, 1673–1679.
Clark, A., Meignin, C., Davis, I., 2007. A Dynein-dependent shortcut rapidly delivers axis determination transcripts into the *Drosophila* oocyte. Development 134, 1955–1965.
Claußen, M., Koch, R., Jin, Z.Y., Suter, B., 2006. Functional characterization of *Drosophila Translin and Trax*. Genetics 174, 1337–1347.
Claußen, M., Suter, B., 2005. BicD-dependent localization processes: from *Drosophilia* development to human cell biology. Ann. Anat. 187, 539–553.
Clouse, K.N., Ferguson, S.B., Schupbach, T., 2008. Squid, Cup, and PABP55B function together to regulate gurken translation in *Drosophila*. Dev. Biol. 313, 713–724.
Coll, O., Villalba, A., Bussotti, G., Notredame, C., Gebauer, F., 2010. A novel, noncanonical mechanism of cytoplasmic polyadenylation operates in *Drosophila* embryogenesis. Genes Dev. 24, 129–134.
Dienstbier, M., Boehl, F., Li, X., Bullock, S.L., 2009. Egalitarian is a selective RNA-binding protein linking mRNA localization signals to the dynein motor. Genes Dev. 23, 1546–1558.
Du, T.G., Schmid, M., Jansen, R.P., 2007. Why cells move messages: the biological functions of mRNA localization. Semin. Cell Dev. Biol. 18, 171–177.
Ephrussi, A., Dickinson, L.K., Lehmann, R., 1991. *oskar* organizes the germ plasm and directs localization of the posterior determinant *nanos*. Cell 66, 37–50.
Gerber, A.P., Luschnig, S., Krasnow, M.A., Brown, P.O., Herschlag, D., 2006. Genome-wide identification of mRNAs associated with the translational regulator PUMILIO in *Drosophila melanogaster*. Proc. Natl. Acad. Sci. U. S. A. 103, 4487–4492.
Gilbert, W.V., Zhou, K., Butler, T.K., Doudna, J.A., 2007. Cap-independent translation is required for starvation-induced differentiation in yeast. Science 317, 1224–1227.
Godt, D., Tepass, U., 1998. *Drosophila* oocyte localization is mediated by differential cadherin-based adhesion. Nature 395, 387–391.
Gorgoni, B., Gray, N.K., 2004. The roles of cytoplasmic poly(A)-binding proteins in regulating gene expression: a developmental perspective. Brief. Funct. Genomic Proteomic 3, 125–141.
Hachet, O., Ephrussi, A., 2001. *Drosophila* Y14 shuttles to the posterior of the oocyte and is required for *oskar* mRNA transport. Curr. Biol. 11, 1666–1674.
Hoogenraad, C.C., Akhmanova, A., Howell, S.A., Dortland, B.R., De Zeeuw, C.I., Willemsen, R., Visser, P., Grosveld, F., Galjart, N., 2001. Mammalian Golgi-associated Bicaudal-D2 functions in the dynein–dynactin pathway by interacting with these complexes. EMBO J. 20, 4041–4054.
Hughes, S.C., Krause, H.M., 1999. Single and double FISH protocols for *Drosophila*. Methods Mol. Biol. 122, 93–101.
Jenny, A., Hachet, O., Zavorszky, P., Cyrklaff, A., Weston, M.D., Johnston, D.S., Erdelyi, M., Ephrussi, A., 2006. A translation-independent role of oskar RNA in early *Drosophila* oogenesis. Development 133, 2827–2833.
Kahvejian, A., Svitkin, Y.V., Sukarieh, R., M'Boutchou, M.N., Sonenberg, N., 2005. Mammalian poly(A)-binding protein is a eukaryotic translation initiation factor, which acts via multiple mechanisms. Genes Dev. 19, 104–130.

Kelsey, C.M., Ephrussi, A., 2009. mRNA localization: gene expression in the spatial dimension. Cell 136, 719–730.
Khaleghpour, K., Kahvejian, A., De Crescenzo, G., Roy, G., Svitkin, Y.V., Imataka, H., O'Connor-McCourt, M., Sonenberg, N., 2001. Dual interactions of the translational repressor Paip2 with poly(A) binding protein. Mol. Cell. Biol. 21, 5200–5213.
Kim-Ha, J., Kerr, K., Macdonald, P.M., 1995. Translational regulation of *oskar* mRNA by Bruno, an ovarian RNA-binding protein, is essential. Cell 81, 403–412.
Kim-Ha, J., Smith, J.L., Macdonald, P.M., 1991. *oskar* mRNA is localized to the posterior pole of the *Drosophila* oocyte. Cell 66, 23–35.
Koch, E.A., Spitzer, R.H., 1983. Multiple effects of colchicine in oogenesis in *Drosophila*: induced sterility and switch of potential oocyte to nurse-cell developmental pathway. Cell Tissue Res. 228, 21–32.
Koch, R., Ledermann, R., Urwyler, O., Heller, M., Suter, B., 2009. Systematic functional analysis of Bicaudal-D serine phosphorylation and intragenic suppression of a female sterile allele of BicD. PLoS One 4, e4552.
Kugler, J.M., Lasko, P., 2009. Localization, anchoring and translational control of *oskar*, *gurken*, *bicoid* and *nanos* mRNA during *Drosophila* oogenesis. Fly (Austin) 3, 15–28.
Lantz, V., Ambrosio, L., Schedl, P., 1992. The *Drosophila orb* gene is predicted to encode sex-specific germline RNA-binding proteins and has localized transcripts in ovaries and early embryos. Development 115, 75–88.
Larsen, K.S., Xu, J., Cermelli, S., Shu, Z., Gross, S.P., 2008. BicaudalD actively regulates microtubule motor activity in lipid droplet transport. PLoS One 3, e3763.
Lemay, J.F., D'Amours, A., Lemieux, C., Lackner, D.H., St-Sauveur, V.G., Bahler, J., Bachand, F., 2010. The nuclear poly(A)-binding protein interacts with the exosome to promote synthesis of noncoding small nucleolar RNAs. Mol. Cell 37, 34–45.
Lemieux, C., Bachand, F., 2009. Cotranscriptional recruitment of the nuclear poly(A)-binding protein Pab2 to nascent transcripts and association with translating mRNPs. Nucleic Acids Res. 37, 3418–3430.
Li, X., Kuromi, H., Briggs, L., Green, D.B., Rocha, J.J., Sweeney, S.T., Bullock, S.L., 2010. Bicaudal-D binds clathrin heavy chain to promote its transport and augments synaptic vesicle recycling. EMBO J. 29, 992–1006.
Libri, D., 2010. Nuclear poly(a)-binding proteins and nuclear degradation: take the mRNA and run? Mol. Cell 37, 3–5.
Lin, M.D., Fan, S.J., Hsu, W.S., Chou, T.B., 2006. *Drosophila* decapping protein1, dDcp1, is a component of the oskar mRNP complex and directs its posterior localization in the oocyte. Dev. Cell 10, 601–613.
Mach, J., Lehmann, R., 1997. An Egalitarian–BicaudalD complex is essential for oocyte specification and axis determination in *Drosophila*. Genes Dev. 11, 423–435.
Mangus, D.A., Evans, M.C., Jacobson, A., 2003. Poly(A)-binding proteins: multifunctional scaffolds for the post-transcriptional control of gene expression. Genome Biol. 4, 223.
Markussen, F., Michon, A., Breitwieser, W., Ephrussi, A., 1995. Translational control of oskar generates short OSK, the isoform that induces pole plasma assembly. Development 121, 3723–3732.
Melo, E.O., Dhalia, R., Martins de Sa, C., Standart, N., de Melo Neto, O.P., 2003. Identification of a C-terminal poly(A)-binding protein (PABP)–PABP interaction domain: role in cooperative binding to poly (A) and efficient cap distal translational repression. J. Biol. Chem. 278, 46357–46368.
Mohler, J., Wieschaus, E., 1986. Dominant maternal-effect mutations of *Drosophila melanogaster* causing the production of double-abdomen embryos. Genetics 112, 803–822.
Mohr, E., Richter, D., 2004. Subcellular vasopressin mRNA trafficking and local translation in dendrites. J. Neuroendocrinol. 16, 333–339.
Mohr, E., Fuhrmann, C., Richter, D., 2001a. VP-RBP, a protein enriched in brain tissue, specifically interacts with the dendritic localizer sequence of rat vasopressin mRNA. Eur. J. Neurosci. 13, 1107–1112.
Mohr, E., Prakash, N., Vieluf, K., Fuhrmann, C., Buck, F., Richter, D., 2001b. Vasopressin mRNA localization in nerve cells: characterization of cis-acting elements and trans-acting factors. Proc. Natl. Acad. Sci. U. S. A. 98, 7072–7079.
Mohr, S.E., Dillon, S.T., Boswell, R.E., 2001c. The RNA-binding protein Tsunagi interacts with Mago Nashi to establish polarity and localize oskar mRNA during *Drosophila* oogenesis. Genes Dev. 15, 2886–2899.
Navarro, C., Puthalakath, H., Adams, J.M., Strasser, A., Lehmann, R., 2004. Egalitarian binds dynein light chain to establish oocyte polarity and maintain oocyte fate. Nat. Cell Biol. 6, 427–435.
Newmark, P.A., Boswell, R.E., 1994. The mago nashi locus encodes an essential product required for germ plasm assembly in *Drosophila*. Development 120, 1303–1313.
Oh, J., Steward, R., 2001. Bicaudal-D is esscential for egg chamber formation and cytoskeletal organization in *Drosophila* oogenesis. Dev. Biol. 232, 91–104.
Palacios, I.M., Gatfield, D., St Johnston, D., Izaurralde, E., 2004. An eIF4AIII-containing complex required for mRNA localization and nonsense-mediated mRNA decay. Nature 427, 753–757.
Pare, A., Lemons, D., Kosman, D., Beaver, W., Freund, Y., McGinnis, W., 2009. Visualization of individual Scr mRNAs during *Drosophila* embryogenesis yields evidence for transcriptional bursting. Curr. Biol. 19, 2037–2042.
Parker, R., Song, H., 2004. The enzymes and control of eukaryotic mRNA turnover. Nat. Struct. Mol. Biol. 11, 121–127.
Patel, G.P., Ma, S., Bag, J., 2005. The autoregulatory translational control element of poly (A)-binding protein mRNA forms a heteromeric ribonucleoprotein complex. Nucleic Acids Res. 33, 7074–7089.
Pestova, T.V., Lorsch, J.R., C., H., 2007. The mechanism of translation initiation in eukaryotes. Cold Spring Harbor Laboratory Press, Cold Spring Harbor, N. Y.
Ran, B., Bopp, R., Suter, B., 1994. Null alleles reveal novel requirement for Bic-D during *Drosophila* oogenesis and zygotic development. Development 120, 1233–1242.
Roy, G., Miron, M., Khaleghpour, K., Lasko, P., Sonenberg, N., 2004. The *Drosophila* poly (A) binding protein-interacting protein, dPaip2, is a novel effector of cell growth. Mol. Cell. Biol. 24, 1143–1154.
Schultz, A., Nottrott, S., Hartmuth, K., Lührmann, R., 2006. RNA structural requirements for the association of the spliceosomal hPrp31 Protein with the U4 and U4atac small nuclear ribonucleoproteins. J. Biol. Chem. 281, 28278–28286.
Schüpbach, T., Wieschaus, E., 1991. Female sterile mutations on the second chromosome of *Drosophila melanogaster*: II Mutations blocking oogenesis or altering egg morphology. Genetics 129, 1119–1136.
Sigrist, S., Thiel, P., Reiff, D., Lachance, P., Lasko, P., Schuster, C., 2000a. Postsynaptic translation affects the efficacy and morphology of neuromuscular junctions. Nature 405, 1062–1065.
Sigrist, S.J., Thiel, P.R., Reiff, D.F., Lachance, P.E., Lasko, P., Schuster, C.M., 2000b. Postsynaptic translation affects the efficacy and morphology of neuromuscular junctions. Nature 405, 1062–1065.
Skabkina, O.V., Skabkin, M.A., Popova, N.V., Lyabin, D.N., Penalva, L.O., Ovchinnikov, L.P., 2003. Poly(A)-binding protein positively affects YB-1 mRNA translation through specific interaction with YB-1 mRNA. J. Biol. Chem. 278, 18191–18198.
St Johnston, D., Beuchle, D., Nüsslein-Volhard, C., 1991. *Staufen*, a gene required to localize maternal RNAs in the *Drosophila* egg. Cell 66, 51–63.
Suter, B., Steward, R., 1991. Requirement for phosphorylation and localization of the Bicaudal-D protein in *Drosophila* oocyte differentiation. Cell 67, 917–926.
Swan, A., Nguyen, T., Suter, B., 1999. *Drosophila* Lissencephaly-1 functions with Bic-D and dynein in oocyte determination and nuclear positioning. Nature Cell Biol. 1, 444–449.
Swan, A., Suter, B., 1996. Role of Bicaudal-D in patterning the *Drosophila* egg chamber in mid-oogenesis. Development 122, 3577–3586.
Swift, S., Xu, J., Trivedi, V., Austin, K.M., Tressel, S.L., Zhang, L., Covic, L., Kuliopulos, A., 2010. A novel protease-activated receptor-1 interactor, Bicaudal D1, regulates G protein signaling and internalization. J. Biol. Chem. 285, 11402–11410.
Tarun Jr., S.Z., Sachs, A.B., 1996. Association of the yeast poly(A) tail binding protein with translation initiation factor eIF-4G. EMBO J. 15, 7168–7177.
Theurkauf, W.E., Alberts, B.M., Jan, Y.N., Jongens, T.A., 1993. A central role for microtubules in the differentiation of *Drosophila* oocytes. Development 118, 1169–1180.
Trautwein, M., Dengjel, J., Schirle, M., Spang, A., 2004. Arf1p provides an unexpected link between COPI vesicles and mRNA in Saccharomyces cerevisiae. Mol. Biol. Cell 15, 5021–5037.
Tucker, M., Staples, R.R., Valencia-Sanchez, M.A., Muhlrad, D., Parker, R., 2002. Ccr4p is the catalytic subunit of a Ccr4p/Pop2p/Notp mRNA deadenylase complex in Saccharomyces cerevisiae. EMBO J. 21, 1427–1436.
van Eeden, F.J., Palacios, I.M., Petronczki, M., Weston, M.J., St Johnston, D., 2001. Barentsz is essential for the posterior localization of *oskar* mRNA and colocalizes with it to the posterior pole. J. Cell. Biol. 154, 511–523.
Vardy, L., Orr-Weaver, T.L., 2007. Regulating translation of maternal messages: multiple represion mechanisms. Trends Cell Biol. 17, 547–554.
Wilhelm, J.E., Smibert, C.A., 2005. Mechanism of translational regulation in *Drosophila*. Biol. Cell. 97, 235–252.